AWARD NUMBER: W81XWH-15-1-0165

TITLE: Development of Novel Nonagonist PPAR-Gamma Ligands for Lung Cancer Treatment

PRINCIPAL INVESTIGATOR: Melin Khandekar, M.D., Ph.D.

CONTRACTING ORGANIZATION: Massachusetts General Hospital
Boston, MA 02114-2696

REPORT DATE: OCT 2018

TYPE OF REPORT: FINAL

PREPARED FOR: U.S. Army Medical Research and Materiel Command
Fort Detrick, Maryland 21702-5012

REPORT DOCUMENTATION PAGE

Form Approved
OMB No. 0704-0188

1. REPORT DATE	2. REPORT TYPE	3. DATES COVERED
OCT 2018	Final report	1 Aug 2015 -31 Jul 2018

4. TITLE AND SUBTITLE

Development of Novel Nonagonist PPAR-Gamma Ligands for Lung Cancer Treatment

5a. CONTRACT NUMBER
W81XWH-15-1-0165

5b. GRANT NUMBER

5c. PROGRAM ELEMENT NUMBER

6. AUTHOR(S)
Melin Khandekar, M.D., Ph.D.

E-Mail:mkhandekar@partners.org

5d. PROJECT NUMBER

5e. TASK NUMBER

5f. WORK UNIT NUMBER

7. PERFORMING ORGANIZATION NAME(S) AND ADDRESS(ES)
Massachusetts General Hospital 55 Fruit St. Boston, MA 02114

8. PERFORMING ORGANIZATION REPORT NUMBER

9. SPONSORING / MONITORING AGENCY NAME(S) AND ADDRESS(ES)

U.S. Army Medical Research and Materiel Command
Fort Detrick, Maryland 21702-5012

10. SPONSOR/MONITOR'S ACRONYM(S)

11. SPONSOR/MONITOR'S REPORT NUMBER(S)

12. DISTRIBUTION / AVAILABILITY STATEMENT

Approved for Public Release; Distribution Unlimited

13. SUPPLEMENTARY NOTES

14. ABSTRACT
The overall goal of this grant is to establish the role of non-agonist PPAR-gamma ligands as potential therapeutic candidates for lung cancer. In this grant period, we have built on our gene expression data to show that a PPAR-gamma S273 phosphorylation signature is correlated with response to chemotherapy in lung cancer in publicly available datasets. We have further shown genetically using lung cancer cell lines lacking p53, that p53 is an important mediator of ability of non-agonist PPAR-gamma ligands to sensitize lung cancer to DNA damaging agents. We have demonstrated a biochemical interaction between p53 and PPAR-gamma, which provides insight into the groups of patients for whom this combination therapy may benefit. We have also found new interactions of PPAR-gamma with other players in DNA damage repair, including BRCA1 and gamma-H2AX. We continue to make progress on the other aims of this grant, which aim to test this hypothesis in genetic animal models of lung cancer and to identify novel partners for PPAR-gamma that may play a role in DNA repair.

15. SUBJECT TERMS
PPAR-gamma, lung cancer, gene expression, p53, thiazolidinedione

16. SECURITY CLASSIFICATION OF:			17. LIMITATION OF ABSTRACT	18. NUMBER OF PAGES	19a. NAME OF RESPONSIBLE PERSON
a. REPORT	b. ABSTRACT	c. THIS PAGE			USAMRMC
Unclassified	Unclassified	Unclassified	Unclassified	27	19b. TELEPHONE NUMBER *(include area code)*

TABLE OF CONTENTS

1. **Introduction** **4**
2. **Keywords** **4**
3. **Accomplishments** **11**
4. **Impact** **12**
5. **Changes/Problems** **13**
6. **Products** **14**
7. **Participants and Collaborating Organizations** **14**
8. **Special Reporting Requirements** **NA**
9. **Appendices** **15**

INTRODUCTION

In the veteran population, lung cancer is the number one cause of cancer death. Our previous work demonstrated that ligands for the transcription factor PPARγ, the thiazolidinediones (TZDs), synergized with carboplatin treatment of lung cancer in vitro and in vivo. Unfortunately, the use of TZDs has declined as the adverse effects of these drugs have come to light. Recently, we have demonstrated that novel PPARγ ligands that lack any agonist activity, but inhibit phosphorylation of pS273 are effective anti-diabetic agents that lack many side effects caused by TZD treatment. To generate novel therapeutics with potential in lung cancer, we have explored the role of these non-agonist PPARγ ligands in cancer treatment. We have demonstrated that there is robust phosphorylation of PPARγ after carboplatin treatment in A549 cells, which can be inhibited by non-agonist ligands (NALs). These drugs are active in vitro and in vivo in genetic mouse models and xenografts. In this work, we are exploring the role of PPARγ ligands in lung cancer treatment by identifying biomarkers of activity, mechanisms of action and validating their role in genetic models of lung cancer. We have generated a gene set representative of the activity of these agonist ligands in combination with carboplatin. We have identified p53 signaling as a key mediator of the ability of these non-agonist ligands ability to sensitize cells to carboplatin. Given the broad importance of this pathway in the DNA damage response, we have also shown that non-agonist PPARγ ligands are able to sensitize lung cancer to a wide variety of DNA damaging agents, which further broadens the potential clinical applications of this line of inquiry. We anticipate this will develop a new avenue to combine anti-diabetic drugs and cancer therapy and will lead to a significant improvement in overcoming treatment resistance or chemoprevention of lung cancer death for veterans

KEYWORDS

PPAR-gamma; Lung cancer; DNA damage response; Thiazolidinediones; p53

ACCOMPLISHMENTS

Aim 1 / Major Task 1: Generate gene set altered by carboplatin treatment with and without inhibition of pS273 phosphorylation.

One of the goals of the project was to generate a gene set representative of the inhibition of pS273 phosphorylation after carboplatin treatment. To accomplish this task, we turned to Affymetrix gene expression profiling. To get the purest representation of this gene set, we generated fibroblasts from the brown adipose tissue of mice with the S273→A mutation or wild type *Pparg* (*Pparg*$^{KI/KI}$ or *Pparg*$^{+/+}$) (Appendix Supplemental Figure S1F.) We immortalized these cells using retrovirus expressing the SV40 Large T antigen. We treated these cells with increasing doses of carboplatin and demonstrated that this model recapitulates the effects of non-agonist ligand treatment, as there is a significant increase in markers of cell death including cleaved PARP1 and cleaved Caspase 3 in cells with the S273A mutation (Appendix Figure 1.)

To assess the genetic changes induced by inhibiting the phosphorylation of PPARγ, we used unbiased gene expression profiling using Affymetrix arrays. RNA from *Pparg*$^{+/+}$ and *Pparg*$^{KI/KI}$ fibroblasts treated with 25μM carboplatin or saline were harvested and

hybridized to arrays. The resulting gene expression data was analyzed and unbiased hierarchical clustering revealed that the samples segregated according to genotype and then by treatment with carboplatin (Appendix Figure 2A). Examination of volcano plots revealed that at baseline, 187 genes were significantly downregulated more than 2-fold in the mutant cells, and 67 genes were upregulated. Upon treatment with carboplatin, the differences between the genotypes was much more prominent, with 395 genes downregulated in mutant cells and 215 genes upregulated. The greater difference in gene expression between these two genotypes upon treatment with carboplatin is consistent with the idea that S273 phosphorylation is a critical event in response to carboplatin treatment, and inhibition of this phosphorylation by changing a single amino acid results in a profound change in the transcriptome of the cells.

We subsequently validated these gene expression changes using QPCR from cDNA prepared from wild type and mutant fibroblasts cultures in the presence or absence of carboplatin (Appendix Supplement Figure S2A.) We selected a group of genes that were at least 3-fold upregulated with an ANOVA p value <0.5. A total of 59 genes (excluding predicted genes and uncharacterized cDNAs) met these criteria and were analyzed (Appendix Figure 1C). Forty of these were significantly ($p<0.05$) regulated in separate experiments (chi-square $p<0.0063$) and multiple others trended towards significance.

To examine whether similar changes were seen in the lung cancer cell lines in which PPARγ phosphorylation has been inhibited, we examined the expression of these genes in other cell types to generate a core signature of PPARγ phosphorylation inhibition after carboplatin treatment (Appendix Supplement Figure S2B.) A core set of genes was generated based on their expression in multiple cell types with and without carboplatin treatment. A set of 12 genes that were upregulated in the S273A mutant and 11 genes that were downregulated in the S273A mutant were assessed in A549 cells treated with the non-agonist ligand SR1664 in combination with carboplatin (Appendix Figure 2B). Ten of the 12 upregulated genes were coordinately upregulated in A549 cells treated with SR1664 and carboplatin. Seven of the 11 genes were appropriately downregulated with SR1664 treatment with carboplatin, for a total of 17/23 genes appropriately regulated (chi square $p=0.0218$.) This core gene set represents gene expression based readout of the inhibition of PPARγ phosphorylation in response to carboplatin.

To assess for potential mechanisms of the increased sensitivity to genotoxic drugs, we performed Gene Set Enrichment Analysis using the microarray data generated from wild type and S273A mutant fibroblasts treated with carboplatin with the Hallmark gene sets (Appendix Figure 4A.) The most enriched gene set associated with S273A mutation was the p53 pathway (Appendix Supplement Figure S4C). Interestingly, several other pathways involving the DNA damage response were upregulated, including the UV response, and DNA repair pathways, although the FDR q-value was >0.05 for these sets. This analysis raises the intriguing possibility that the single amino acid change in the S273A knock in mutants that eliminates phosphorylation results in alteration of certain aspects of the DNA damage response.

Given the critical role that p53 plays in the response both to DNA damage and the initiation of apoptosis, we hypothesized that the interaction of p53 and PPARγ may play an important role in the ability of non-agonist PPARγ ligands to sensitize cancer cells to the cytotoxic effects of carboplatin. We examined the effects of a non-agonist PPARγ ligand in combination with carboplatin in Calu-1 cells, which have a genetic deletion of p53 (Appendix Supplement Figure S4F lanes 1-6,) as well as H2009 cells, which express mutant p53 (Appendix Supplement Figure S4B). In both of these cell types, we fail to see an increase in the DNA damage marker γ-H2AX when cells are treated with both SR1664 and carboplatin. To demonstrate that this lack of sensitization was due to the lack of p53, we ectopically expressed p53 in these cells by transient transfection. Although the H2009 cells died upon introduction of wild type p53, Calu-1 cells expressing wild type p53 showed increased γ-H2AX accumulation when treated with SR1664 and carboplatin (Appendix Supplement Figure S4F, lanes 7-12.) These data suggest that the presence of wild type p53 is required for the sensitizing effects of non-agonist PPARγ ligands.

To further investigate the role of p53 in the ability of non-agonist ligands to sensitize cells to DNA damaging agents, we performed Crispr/Cas9 mediated deletion of TP53 (Appendix Figure 4D) from A549 cells. Control cells transduced with Cas9 alone show robust increases in cleaved PARP and cleaved Caspase 3 when treated with the non-agonist ligand SR10171 and doxorubicin compared to doxorubicin alone (Appendix Figure 4D, lane 3 vs. lane 6.) Contrastingly, cells depleted of p53 show no significant increase in accumulation of apoptotic markers when co-treated with SR10171 and doxorubicin compared to doxorubicin. Additionally, these cells show no increase in γ-H2AX phosphorylation when co-treated with non-agonist ligands and doxorubicin, while the control cells continue to be sensitized. As an alternative approach, we performed shRNA mediated knockdown of TP53 from A549 cells. Lentiviral transduction of A549 cells with a shRNA directed against p53 resulted in significantly decreased p53 accumulation. Control cells infected with a scrambled shRNA continue to show increased γ-H2AX when treated with the non-agonist ligand SR10171 and doxorubicin. Contrastingly, A549 cells that have been depleted of p53 show no increased γ–H2AX accumulation upon co-treatment with doxorubicin and SR10171 (Appendix Supplement Figure S4E). These data suggest that p53 is required for the ability of non-agonist PPARγ ligands to sensitize cells to genotoxic agents.

We then sought to address whether the gene signature we identified was indeed induced in human patients receiving carboplatin and pioglitazone, a traditional PPAR-gamma ligand. We obtained tissue from 7 patients who participated in a clinical trial, DFCI 11-096, a phase I clinical trial of pioglitazone with carboplatin in patients with advanced cancer. In this study, patients were enrolled and given one cycle of carboplatin, followed by one cycle of carboplatin with pioglitazone, which was continued until progression. Biopsies were taken from tumor tissue after the first cycle (carboplatin alone) and second (pioglitazone + carboplatin.) We assessed the biopsy specimens and unfortunately, one patient did not have any tumor in the specimens. Thus, 6 patients had tissue available for analysis.

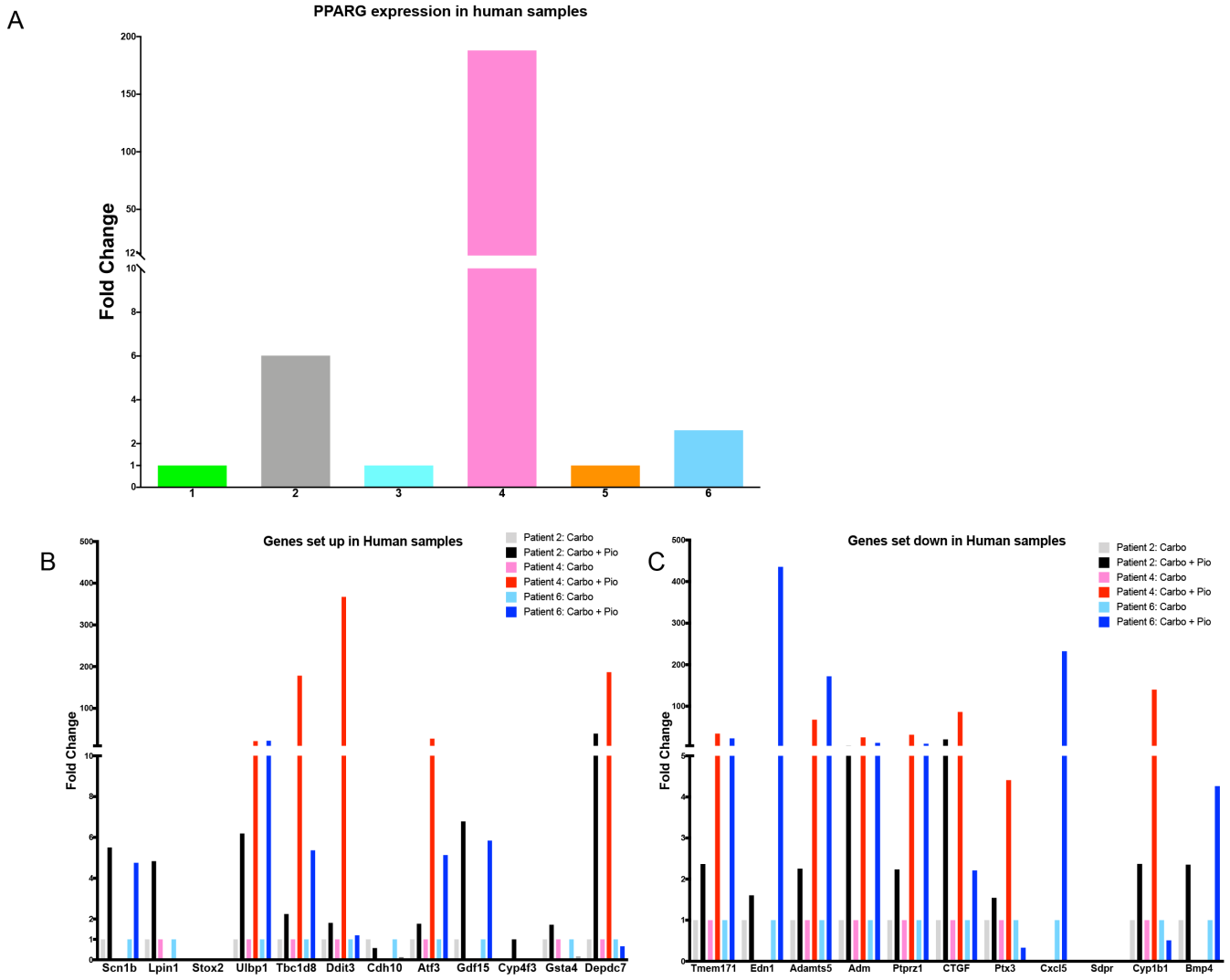

Figure 1: Analysis of gene expression from human patients receiving pioglitazone / carboplatin. A) Expression of PPAR-gamma was very low in 3 samples, while 3 had more detectable levels. B) Genes in the upregulated gene set were generally also upregulated in patient samples. C) Genes in the down regulated gene set did not seem to be coordinately downregulated in human samples.

As seen in Figure 1A, only 3 of these patients had any appreciable expression of PPAR-gamma, as this was not a criterion for eligibility in the study. In retrospect, this test may have helped enrich the number of patients that would have been informative in our analysis. We then examined the expression of our gene set in these 3 patients, pre and post pioglitazone. We did see that the genes that were upregulated in our gene set did seem to be increased after treatment with pioglitazone, however, this trend was not as apparent with the downregulated gene set. Unfortunately, our limited sample size makes statistical analysis impossible. However, it is clear that the combination of pioglitazone and carboplatin is safe, tolerable, and this provides proof of concept of a future clinical trial that could be performed.

As an alternative approach to looking at human data, we queried whether expression of the combined gene set correlated with the outcomes of patients treated with chemotherapy in publicly available gene expression datasets. Patients in the Director's Challenge Consortium who received adjuvant chemotherapy (n=90) and the UT Lung SPORE cohort (n=49), two of the largest cohorts of lung cancer patients receiving adjuvant chemotherapy with available gene expression data, were classified based on their expression of the genes in the signature. Overexpression (as defined by expression greater than the mean of the expression across the cohort) of the upregulated genes and underexpression (expression less than the mean) of the downregulated genes was used to create a signature score by which patients were classified. Kaplan Meier analysis of overall survival in these two combined cohorts showed that patients with greater than median signature score had a trend towards better survival than those who did not express the signature (p=0.097) (Appendix Figure 2C.) Analysis of these studies separately showed a similar trend when analyzed as a individually as well (p=0.1 and p=0.34 Figure S3C.)

We examined a separate cohort of patients, we used the KMplot online tool (www.kmplotter.com) to examine whether this gene set was associated with chemotherapy outcome in other cohorts. A multigene classifier dividing groups based on mean gene expression (with equal weighting of all the genes and with negative weighting of downregulated genes) showed that patients with lung cancer treated with chemotherapy showed a trend for improved outcomes with a hazard ratio of 0.27 (p=0.0507) (Appendix Supplementary Figure S2D), although the analysis was limited by a small number of patients (n=34). Furthermore, we demonstrated in the cohort of lung cancer patients not receiving chemotherapy that there was no association of the genetic signature with survival (Appendix Supplementary Figure 2E). This suggests that the gene set is specifically predictive of the effects of the response to chemotherapy, rather than a purely prognostic biomarker. Of course, all of these analyses are limited due to the mixed clinical and pathologic features of these cohorts of patients. However, these data suggest that low expression of the downregulated genes and high expression of the upregulated genes is associated with improved outcomes among patients receiving systemic chemotherapy.

Aim 2 / Major task 1: Immunoprecipitation of PPARγ from cells treated with and without carboplatinum and non-agonist PPARγ ligands.

One of the goals of this project was to use an unbiased approach to purify a complex of phosphorylated and non-phosphorylated PPARγ in the presence and absence of carboplatin. We first attempted to purify endogenous PPAR-gamma from fibroblasts from the knock-in mice, which was our initial preferred approach, as this would accurately reflect binding partners at endogenous levels of PPAR-gamma. Unfortunately, the levels of PPAR-gamma were insufficient to immunoprecipitate sufficient quantity of protein for analysis.

Our next approach was to retrovirally express PPAR-gamma in H460 lung cancer cells, which do not express significant amounts of PPARγ. We then expressed either wild

type PPARγ or S273A mutant PPARγ, and we were able to identify conditions that resulted in good purity of protein (Appendix Figure 2A.) However, as we expanded these clones to produce larger quantities of protein, we ultimately found that the expression of PPAR-gamma was reduced. We believe that forced expression of PPAR-gamma results in slowing of the cell cycle, which favors cells that suppress PPAR-gamma expression during proliferation via genetic or epigenetic mechanisms. Thus, expansion of these cells results in low amounts of PPAR-gamma compared to our test batches, limiting our ability to purify sufficient quantities of PPAR-gamma to use for mass spectrometry analysis

To circumvent this limitation, we next generated new constructs that express either wild type or S273A mutant PPAR-gamma using adenoviral vectors that can be used to generate high level transient expression of PPAR-gamma in large numbers of cells. We used the Gateway Cloning System to introduce human PPAR-gamma1 into an adenoviral vector with a V5 protein tag for purification. We have been able to express and IP the PPAR-gamma protein from both of these as seen in Figure 2 panel B. We are now infecting larger numbers of cells with these constructs, and although the grant period is now closed, we anticipate being able to obtain these data in the near future.

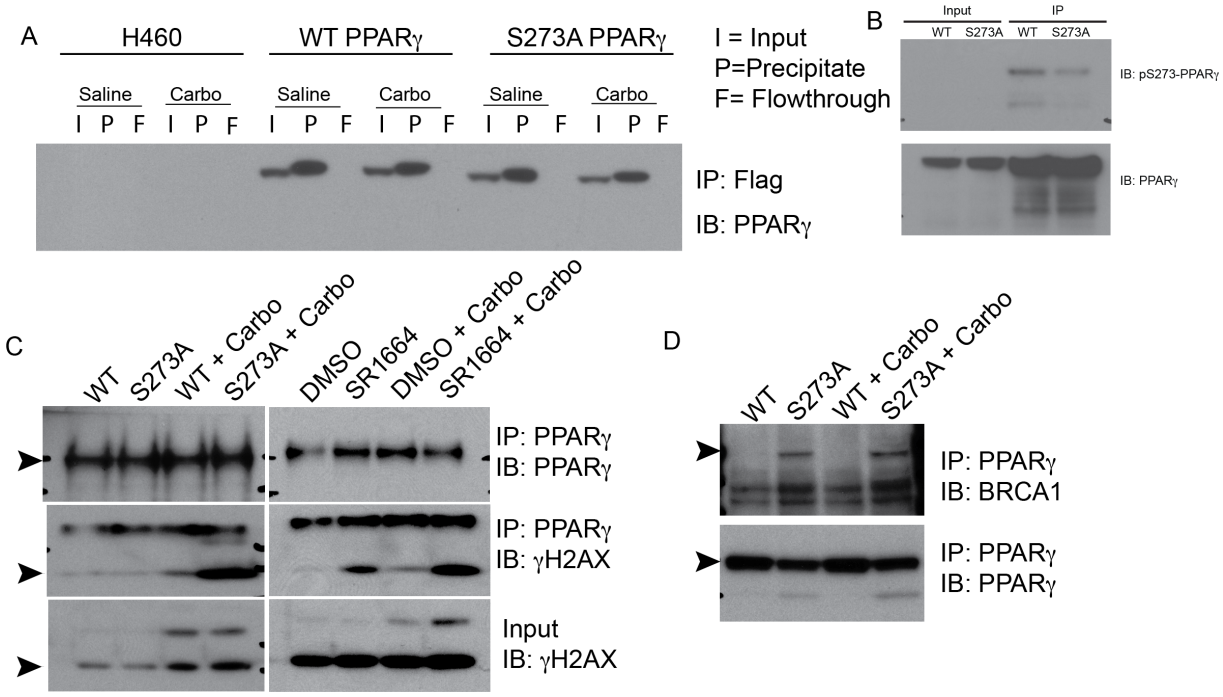

Figure 2: Protein purification scheme for PPAR-gamma. A) Initial purification schema from retrovirally expressed PPAR-gamma in H460 cells. B) Newer purification strategy using adenovirally expressed PPAR-gamma in E0771 cells. C) Dynamic association of PPAR-gamma and g-H2AX is disrupted by S273A phosphorylation, similar to p53. D) Association of PPAR-gamma with BRCA1 is disrupted by phosphorylation.

Aim2/ Major task 2: Assess protein complex members for function in response to carboplatin.

Although we are still working on our unbiased mass spectrometry approach to yield results, as an alternative approach, I had proposed targeted immunoprecipitation experiments to explore potential candidates that may play a functional role in the sensitization of lung cancer cells to non-agonist ligands.

Given the effects on the p53 gene set, we hypothesized that there may be a biochemical interaction between p53 and PPARγ. Immunoprecipitation of PPARγ from nuclear extracts of WT or S273A mutant fibroblasts followed by immunoblotting for p53 demonstrates that the wild type PPARγ physically associates with p53 while the S273A mutant does not (Appendix Figure 4B.) This is true both in the presence and the absence of carboplatin, although there is increased association of p53 upon carboplatin treatment. There is no difference in the total levels of PPARγ, and no difference in nuclear accumulation of PPARγ (Appendix Supplement Figure S4B.). These data suggest that phosphorylation of PPARγ stabilizes the interaction of PPARγ and p53, and that mutant PPARγ that cannot be phosphorylated is not able to associate with p53 as efficiently. This differential interaction provides a potential mechanism whereby the blocking the phosphorylation of PPARγ with NALs reduces the interaction with P53 and potentiates apoptotic cell death.

Meanwhile, we have also shown that PPARγ differentially associates with other important proteins in the DNA damage response. We performed immunoprecipitation of PPARγ from nuclear extracts of WT or mutant fibroblasts in the presence and absence of carboplatin. Immunoblotting for γ-H2AX demonstrates that the wild type PPARγ associates less strongly with phosphorylated PPARγ than with the unphosphorylated S273A form. This was also the case in nuclear extracts of A549 cells treated with SR1664, where phosphorylation is inhibited (Figure 2C). These data suggest that upon DNA damage, unphosphorylated PPARγ binds to γ-H2AX, which then dissociates upon S273 phosphorylation. The exact time course of this interaction will need to be explored more fully. We are also examining the potential functional consequences of this interaction using a similar loss of function approach as described above.

Using a similar approach, we have also found that the DNA damage associated protein BRCA1 is associated with PPARγ (Appendix Figure 2C.) Immunoprecipitation of PPARγ from nuclear extracts of WT and knock in mutant fibroblasts followed by analysis by Western blotting, shows that BRCA1 associates with PPARγ S273A more than the WT protein both before and after carboplatin treatment. Again, we are in the process of examining whether this interaction is functionally important using a loss of function approach as described above.

Overall, these data suggest that phosphorylated PPAR-gamma exists in a complex with P53, g-H2AX, and BRCA1, and that inhibition of PPAR-gamma phosphorylation disrupts this complex. We hypothesize that this PPAR-gamma complex assists or enables these proteins to perform their important DNA repair functions, and that disruption of this complex by inhibition of phosphorylation is the major mechanism of action of these drugs.

AIM 3 / Major task 1 and 2: Mouse studies with KRAS mouse and mouse studies with KRAS/LKB1 mice.

Our goal was to test the potential effects of PPAR-gamma S273 phosphorylation on development and treatment of KRAS inducible lung cancer. Unfortunately, our work on this aim has suffered significant delays related to mouse breeding and tumor induction. Specifically, it took significantly longer to obtain mice with the PPAR-gamma S273A homozygous mutation than expected due to demands on the animals for these animals for other experiments in the group. In retrospect, our timeline for performing these experiments was too optimistic.

Once these animals were made, we attempted to induce tumors using adenoviral Cre, and this was another unfortunate source of delays, as our attempts to induce tumors with intranasal administration of adenoviral Cre resulted in significant variability in tumor induction, with the majority of animals not developing lung tumors. On further reflection, our belief is that intranasal administration may have resulted in most of the Cre virus getting displaced into the nasal or oral cavity rather than being delivered into the deep lung tissue. This may have been due to shallow breathing under anesthesia. Given the long latency of the KRAS model to tumor development, this resulted in significant delays, and as such, the work is ongoing. We do anticipate completing this experiment, although the period of the grant is now closed. To ensure such an event does not occur again, we will collaborate with a group that has experience with intratracheal administration of Cre, as this is felt to be much more reliable than intranasal administration (Dupage et al, Nature Protocols 2009.) As such, we are re-establishing these cohorts and attempt the experiment again.

Training and Professional Development Opportunities

This project has provided a number of opportunities for training. I have had the opportunity to attend weekly clinical conferences as well as monthly research conferences. I was also able to present my work at the Spiegelman Lab group meeting, and get feedback from a group of scientists with expertise in a diverse group of fields. This work was presented several times during monthly joint lab meetings with Dr. Pere Puigserver, Professor of Cell Biology at Harvard Medical School and Dr. Evan Rosen, Professor of Medicine at Harvard Medical school and their groups. I received valuable feedback from these presentations. I met with Dr. Spiegelman, my mentor, at least twice a month to review data and discuss scientific issues and directions. An abstract based on this work was accepted as a poster presentation at the Keystone Symposium Conference: New Frontiers in Understanding Tumor Metabolism. I was also invited to present this work at the Obesity Cancer Working Group in New York City, a collaboration between Weill Cornell Medical School, Memorial Sloan Kettering Cancer Institute, and Rockefeller University. I was also invited to present this work in the Steele Laboratories of Tumor Biology at Massachusetts General Hospital.

During the time of this award, I was able to develop my career further by applying for promotion from Instructor to Assistant Professor at Harvard Medical School. I will have the opportunity moving forward to start my own research group at the Massachusetts General Hospital.

Dissemination of Results

We published a paper describing our results in the *Proceedings of the National Academy of Science USA*. The paper was promoted in a press release from the Dana Farber Cancer Institute (https://www.dana-farber.org/newsroom/news-releases/2018/novel-diabetes-drugs-sensitize-cancer-cells-to-chemotherapy-agents/), and the DOD's CDRMP web page (cdmrp.army.mil/lcrp/research_highlights/18khandekar_highlight).

Plans for Next Year

Nothing to report formally as the period of the award will be ended, although we plan to complete the aims outlined in this grant that have not yet been achieved, despite the delays that we had in our extended timeline.

IMPACT

We have now published our paper as described above, and had some press releases regarding the findings of the award. We were able to secure meetings with pharmaceutical companies (both traditional pharma as well as smaller biotech companies) regarding the possibility of adapting non-agonist ligands, traditional TZD PPAR-gamma ligands, or novel chemical matter that these companies were using to use in cancer directed research. Unfortunately, we had some pushback regarding further development of drugs in the PPAR-gamma pathway due to the prior black box warning on rosiglitazone, although it is acknowledged that those findings were likely spurious. Furthermore, we argued that all the previous trials performed with PPAR-gamma ligands have been performed without biomarker selection (e.g. PPAR-gamma expression), and thus is ripe for further testing. We are exploring using pioglitazone in a larger prospective trial in combination with chemotherapy, although securing funding for this type of work is limited by the fact that pioglitazone is no longer on patent, limiting drug company interest in such a trial.

The most serious limitation on the translation of the work stems from a large change in the treatment of metastatic lung cancer, namely the rise of immune checkpoint blockade as a key part of the backbone of systemic therapy for lung cancer. However, we believe that these drugs, by inhibiting aspects of DNA repair, may promote neoantigen formation and may increase the likelihood of these drugs working with platinum agents when combined with immunotherapy. This is another area of interest for further work developing these drugs for lung cancer.

This work does have implications for other disciplines as well. We have shown the ability of these drugs to modulate PPARγ activity in lung cancer, and data from our paper show similar findings in triple negative breast cancer cell lines, as well as association of our genetic signature with outcomes in breast cancer patients. Furthermore, we hope that demonstration of the relative safety of these non-agonist ligands in cancer may propel them to be explored as anti-diabetic agents for metabolic disease as well.

Our data describing the physical interaction between p53 and PPARγ is novel, and may suggest that PPARγ has a role in modifying p53 function in other tissues. It has been shown that p53 plays an important role in metabolism and adipose tissue function, and this may be modulated by PPARγ expression as well.

At this point, I do not have anything to report regarding potential impacts on technology transfer or on society beyond science and technology as a whole.

CHANGES/PROBLEMS

Changes in approach: Rather than intranasal Cre administration, we are planning to use intra-tracheal administration as a method to ensure more uniform tumor formation within the cohorts.

Actual or anticipated problems or delays: Unfortunately, we had several delays which have limited the progress in our aims, and in retrospect the three aims may have been overly ambitious to accomplish.

First, for Aim 1, we had some difficulty obtaining specific IRB approval for our study, largely due to coordination and communication issues around using tissues obtained in one protocol to be used for analysis in the genetic signature. We did obtain this approval in the past year, and were able to perform the analysis described above. Ultimately, the accrual to the study was limited, likely due to the requirement for 2 biopsies for the translational studies. Furthermore, because the study did not look at PPAR-gamma expression prior to accrual, a number of the patients enrolled in the study did not have significant PPAR-gamma expression in the tumors. Thus, these tumors would not be responsive to the PPAR-gamma ligands, and thus are not relevant to this analysis. We were able to look at pre and post pioglitazone specimens from 3 patients, although the statistical power is limited.

For Aim 2, it has longer than anticipated to find appropriate conditions to immunoprecipitate an amount of PPARγ protein from these cells sufficient for mass spectrometric analysis. Although we found good conditions for purity of the immunoprecipitation, our approach of retroviral expression resulted in low levels of protein that were not sufficient to produce a large quantity of PPAR-gamma for mass spectrometric analysis. We then had to derive new vectors to express the protein, using adenoviral tagging and purification. However, we have been able to take a targeted approach to identify multiple members (γ: p53, γ-H2AX, and BRCA1) of a protein complex with PPAR-gamma, all of which play a role in DNA repair. As described above, at least one of these, P53, clearly has a functional role in the effects of PPAR-gamma ligands on sensitivity to DNA damage.

For Aim 3, we have had delays in cohort assembly and tumor induction, which has taken longer than outlined in the SOW. In retrospect, our SOW was too optimistic in terms of the mouse breeding, and we had unanticipated shortages in the S273A knock-in animals for other experiments in the group. Furthermore, our initial cohort tumor induction was insufficient to generate sufficient tumors from the animals for analysis, and we believe that intratracheal administration of Cre may be required to result in adequate tumor induction to study the question. However, both Dr. Spiegelman and I are committed to complete the work outlined in the grant despite the

term of the grant expiring, as the experiments outlined will help continue to develop these PPAR-gamma ligands as attractive therapeutic candidates in cancer.

Changes that had impact on expenditures: We did not have material changes to the budget. My research mentor covered the animal costs as there was a lot of difficulty in using my funds based at the MGH to purchase animals, which are in the BIDMC Animal Faciilty, and there is no ongoing relationship between those groups as there is between the DFCI and BIDMC under Dr. Spiegelman's current arrangement.

Changes in use of human/animals: Nothing to report

PRODUCTS

Publications, conference papers, and presentations.

Poster Presentation: Melin J. Khandekar, Alex S. Banks, Dina Laznik-Bogoslavski, James P. White, Jang H. Choi, Kwok-kin Wong, Ted Kamenecka, Patrick R. Griffin, Bruce M. Spiegelman. "Non-agonist PPAR-gamma ligands sensitize cancer cells to the effects of cytotoxic chemotherapy by inhibiting phosphorylation of Serine 273 and modulating the response to DNA damage." New Frontiers in Understanding Tumor Metabolism, Banff, Canada. February 2016

Invited Oral Presentation: Selective modulation of PPAR-gamma influences the response of cells to DNA damage and potentiates cytotoxic therapy. Obesity and Cancer Working Group Meeting. Memorial Sloan Kettering Cancer Center. New York, NY. March 21, 2016.

Invited Oral Presentation: Selective modulation of PPAR-gamma influences the response of cells to DNA damage and potentiates cytotoxic therapy. Obesity and Cancer Working Group Meeting. Edwin L. Steele Laboratory for Tumor Biology, Massachusetts General Hospital, Boston, MA. November 2016

Manuscript: Khandekar MJ, Banks AS, Laznik-Bogoslavski D, White JP, Choi JH, Kazak, L, Lo JC, Cohen P, Wong KK, Kamenecka TM, Griffin PR, Spiegelman BM. Non-agonist PPAR-gamma ligands modulate the response to DNA damage and sensitize cancer cells to the effects of cytotoxic chemotherapy. PNAS. 2018;115(3):561-566.

PARTICIPANTS

Name:	Melin Khandekar
Role:	PI
Nearest Person Month Worked	16 months
Contribution:	Performed all work described above
Funding Support	No change

Name:	Bruce Spiegelman

Role:	Mentor
Nearest Person Month Worked	NA
Contribution:	Advised PI regarding experimental design, and analysis of experiments
Funding Support	No change

Other Partner Organizations

Name**:** Dana Farber Cancer institute
Location: Boston, MA
Contribution: Facilities and collaboration with mentor's laboratory staff

Name**:** The Scripps Research Institute Florida
Location: Jupiter, FL
Contribution: In kind support (reagents) and collaboration regarding non-agonist ligand dosing

Noncanonical agonist PPARγ ligands modulate the response to DNA damage and sensitize cancer cells to cytotoxic chemotherapy

Melin J. Khandekar[a,b,c], Alexander S. Banks[a,b,1], Dina Laznik-Bogoslavski[a,b], James P. White[a,b,2], Jang Hyun Choi[a,b,3], Lawrence Kazak[a,b], James C. Lo[a,b,4], Paul Cohen[a,b,5], Kwok-Kin Wong[d,6], Theodore M. Kamenecka[e], Patrick R. Griffin[e], and Bruce M. Spiegelman[a,b,7]

[a]Department of Cell Biology, Harvard Medical School, Dana Farber Cancer Institute, Boston, MA 02215; [b]Department of Cancer Biology, Harvard Medical School, Dana Farber Cancer Institute, Boston, MA 02215; [c]Department of Radiation Oncology, Massachusetts General Hospital, Boston, MA 02114; [d]Department of Medical Oncology, Dana Farber Cancer Institute, Boston, MA 02215; and [e]Department of Molecular Therapeutics, The Scripps Research Institute, Jupiter, FL 33458

Contributed by Bruce M. Spiegelman, December 6, 2017 (sent for review October 11, 2017; reviewed by Christopher K. Glass and Mitchell A. Lazar)

The peroxisome-proliferator receptor-γ (PPARγ) is expressed in multiple cancer types. Recently, our group has shown that PPARγ is phosphorylated on serine 273 (S273), which selectively modulates the transcriptional program controlled by this protein. PPARγ ligands, including thiazolidinediones (TZDs), block S273 phosphorylation. This activity is chemically separable from the canonical activation of the receptor by agonist ligands and, importantly, these noncanonical agonist ligands do not cause some of the known side effects of TZDs. Here, we show that phosphorylation of S273 of PPARγ occurs in cancer cells on exposure to DNA damaging agents. Blocking this phosphorylation genetically or pharmacologically increases accumulation of DNA damage, resulting in apoptotic cell death. A genetic signature of PPARγ phosphorylation is associated with worse outcomes in response to chemotherapy in human patients. Noncanonical agonist ligands sensitize lung cancer xenografts and genetically induced lung tumors to carboplatin therapy. Moreover, inhibition of this phosphorylation results in deregulation of p53 signaling, and biochemical studies show that PPARγ physically interacts with p53 in a manner dependent on S273 phosphorylation. These data implicate a role for PPARγ in modifying the p53 response to cytotoxic therapy, which can be modulated for therapeutic gain using these compounds.

PPARγ | DNA damage | lung cancer | chemotherapy

The peroxisome proliferator activator receptor-γ (PPARγ) is an orphan nuclear receptor that is essential for the development of adipocytes (1) and is the target for the thiazolidinedione (TZD) class of antidiabetic agents (2). In addition to its role in metabolism, PPARγ is mutated or overexpressed in certain human cancers (3–6). Despite initial excitement regarding the role of PPARγ ligands in cancer therapy, they were not effective as single agents in advanced epithelial malignancies (7, 8). As an alternative approach, our group has demonstrated that TZDs potently sensitize a variety of cancer cells to the cytotoxic effects of carboplatin (9, 10). The mechanism was thought to be via inhibition of metallothionein gene expression, although other mechanisms were not ruled out (11). While these data suggested that PPARγ ligands may play an important role in cancer therapy, the use of these drugs has declined dramatically due reports concerning toxicity, many of which are now known to have been potentially overstated (12).

Recent data from our group has shown that the pleiotropic effects of PPARγ ligands can be chemically separated into two distinct activities. One relates to the ability of ligands to act as canonical agonists of the nuclear receptor on peroxisome proliferator response elements, which leads to adipogenesis. The second relates to the allosteric inhibition of phosphorylation of the Ser273 (serine 273, S273) residue of PPARγ by a variety of kinases, including CDK5 (13) and ERK1/2 (14). Novel noncanonical agonist ligands (NALs) that only inhibit this phosphorylation event retain much of the antidiabetic activity of TZDs. Intriguingly, many of the known side effects of TZDs, including weight gain, fluid retention, and bone loss are correlated with the agonist properties of TZDs rather than their effect on S273 phosphorylation (15, 16). These data suggest that many of the effects of TZDs previously attributed to their effects as agonists may instead be due to their inhibition of S273 phosphorylation, and raise the

Significance

Peroxisome proliferator-activated receptor-γ (PPARγ) is a transcription factor that plays a central role in the formation of adipose tissue. We show that phosphorylation of a single amino acid of PPARγ alters the response of cells to DNA damaging agents, including multiple types of chemotherapy. Noncanonical agonist PPARγ ligands that block PPARγ phosphorylation sensitize a variety of cancer cell types to these chemotherapeutic agents in vitro and in vivo. We show that PPARγ interacts with the tumor-suppressor p53 in a manner dependent on PPARγ phosphorylation at S273. These data strongly suggest that noncanonical agonist PPARγ ligands, which lack many of the known side effects of classic agonists, should be explored for clinical use in combination with traditional chemotherapy for a variety of malignancies.

Author contributions: M.J.K., T.M.K., P.R.G., and B.M.S. designed research; M.J.K., D.L.-B., J.P.W., J.H.C., L.K., J.C.L., and P.C. performed research; A.S.B., K.-k.W., T.M.K., and P.R.G. contributed new reagents/analytic tools; M.J.K. and B.M.S. analyzed data; and M.J.K. and B.M.S. wrote the paper.

Reviewers: C.K.G., University of California, San Diego; and M.A.L., University of Pennsylvania Perelman School of Medicine.

The authors declare no conflict of interest.

Data deposition: The data reported in this paper have been deposited in the Gene Expression Omnibus (GEO) database, https://www.ncbi.nlm.nih.gov/geo (accession no. GSE107709).

[1]Present address: Department of Medicine, Brigham and Women's Hospital, Boston, MA 02115.

[2]Present address: Department of Medicine, Duke Molecular Physiology Institute, Duke University, Durham, NC 27708.

[3]Present address: Department of Biological Sciences, Ulsan National Institute of Science and Technology, Ulsan 44919, South Korea.

[4]Present address: Department of Medicine, Weill Cornell Medical College, New York, NY 10065.

[5]Present address: Laboratory of Molecular Metabolism, Rockefeller University, New York, NY 10065.

[6]Present address: Department of Medicine, New York University Langone Health, New York, NY 10016.

[7]To whom correspondence should be addressed. Email: Bruce_Spiegelman@dfci.harvard.edu.

This article contains supporting information online at www.pnas.org/lookup/suppl/doi:10.1073/pnas.1717776115/-/DCSupplemental.

question of whether S273 phosphorylation may control other previously unappreciated aspects of PPARγ biology.

The increasing prevalence of metabolic disease and cancer has led to a growing recognition of the mechanistic links shared by these two different diseases (17). The shared biology of obesity, diabetes, and cancer suggest that therapies developed for metabolic disease may be useful in cancer treatment (18, 19) or vice versa (14). One potential application of these therapeutics is to increase the efficacy of cytotoxic treatments in cancer (10, 20, 21). It is critical to note that despite rapid advances in both targeted therapy and immunotherapy, the majority of cancer patients will receive either chemotherapy or radiotherapy during the course of their disease. Thus, enhancing the efficacy of cytotoxic therapy remains a crucial goal for cancer patients.

Here we demonstrate that that PPARγ is phosphorylated in response to DNA damage; this phosphorylation can be inhibited by NALs. We show that inhibition of phosphorylation of PPARγ using chemical or genetic approaches results in dramatic sensitization of cells to DNA-damaging agents. S273 phosphorylation alters the association of PPARγ with the tumor suppressor p53 and impacts its function, which is required for the sensitizing effects of PPARγ ligands. These data suggest that PPARγ plays a more direct role in the cellular response to DNA damaging agents than has been previously demonstrated, and offer a therapeutic approach that can be combined with traditional cancer therapies.

Results

PPARγ Is Phosphorylated on S273 in Response to Carboplatin. To investigate the role of phosphorylation of PPARγ in the response to DNA damage, we assessed whether S273 phosphorylation occurs in cancer cells upon treatment with carboplatin. A549 cells, which have been shown to be sensitized to carboplatin by TZDs (10), were treated with increasing concentrations of carboplatin for 24 h. Western blotting of whole-cell lysates prepared from these cells using an antibody specific for the S273 phosphorylated form of PPARγ (13) revealed a very robust dose-dependent increase in phosphorylated PPARγ (Fig. 1*A*).

We then examined the dynamics of phosphorylation status of PPARγ after carboplatin treatment. PPARγ was immunoprecipitated from A549 lysates at the indicated times and analyzed by immunoblotting with the pS273 phospho-specific antibody. By 8 h there was a striking accumulation of phosphorylated PPARγ, which continued at 24 h posttreatment. As in adipose cells, coincubation of the cells with the NAL SR1664 (16) dramatically reduced the phosphorylation of PPARγ (Fig. 1*B*). These data suggest that PPARγ is indeed phosphorylated in cancer cells in response to carboplatin, and this phosphorylation can be inhibited by NALs.

Inhibition of S273A Phosphorylation with Noncanonical Agonist PPARγ Ligands Results in Increased Cell Death in Response to Multiple Genotoxic Agents. We tested the functional consequences of blocking the phosphorylation of PPARγ using NALs in A549 cells treated with carboplatin. SR1664 significantly increased the cytoxic effects of carboplatin. Two-way ANOVA showed a significant interaction of the drug treatment with carboplatin treatment. (Fig. 1*C*) ($P = 0.0009$). This effect was also seen with the partial agonist MRL-24 and NAL SR1824 (Fig. S1 *A* and *B*). These experiments indicate that agonism of PPARγ is dispensable for the ability of TZDs to sensitize these cancer cells to the cytotoxic effects of carboplatin.

We assessed the relative contributions of apoptosis and growth inhibition by cell cycle arrest to the reduction in total cell numbers. A549 cells treated with rosiglitazone and NALs with and without carboplatin showed a dramatic increase in cleaved poly(ADP-ribose) polymerase 1 (PARP1) (Fig. 1*D*), a key marker of apoptosis. Similarly, analysis of cDNA prepared from the mRNA of these cells showed a significant increase in p53 upregulated modulator of apoptosis (PUMA) mRNA, a key mediator of apoptosis (Fig. S1*C*). Interestingly, apoptosis was

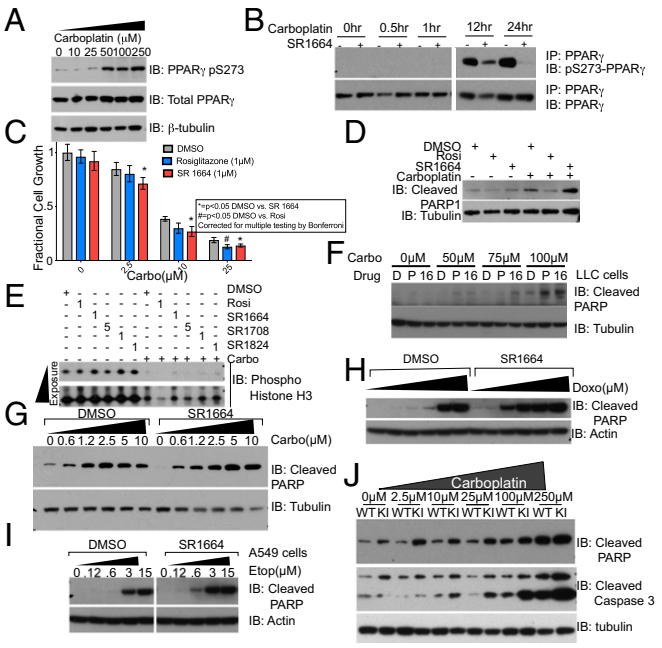

Fig. 1. (*A*) Dose-dependent phosphorylation of PPARγ on S273 with carboplatin treatment. (*B*) Time course of PPARγ phosphorylation as assessed by IP of PPARγ from lysates of A549 cells after treatment with 50 μM carboplatin treated with DMSO or 1 μM SR1664 shows phosphorylation can be inhibited by NALs. IB, immunobot. (*C*) A549 cells treated with increasing concentrations of carboplatin in the presence or absence of either rosiglitazone or SR1664 show equivalent effects on total cell number at 24 h. (*D*) Increased markers of apoptotic cell death with cotreatment of NALs and carboplatin as assessed by immunoblot for cleaved PARP1 (*E*) NALs do not further suppress phospho-Histone H3, a mitotic marker indicative of cell cycle progression. (*F* and *G*) Treatment of other cancer types, including LLC (*F*) and MDA-MB-468 cells, a triple-negative breast cancer cell line (*G*), show similar increased production of cleaved PARP when treated with a combination of SR1664 and carboplatin. (*H* and *I*) A549 cells cotreated with doxorubicin (*H*) or etoposide (*I*) with SR1664 shows an increase in apoptosis. Panels in *I* were taken from the same blot. (*J*) Treatment of wild-type (WT) and knock-in (KI) cells with carboplatin demonstrates a dramatically increased sensitivity of knock-in cells to the cytotoxic effects of carboplatin.

significantly higher in cells treated with the NALs compared with rosiglitazone (Fig. 1*D*).

We next examined the induction of cell cycle arrest by studying the phosphorylation of histone H3, a key mitotic marker (Fig. 1*E*). As expected, carboplatin significantly induces cell cycle arrest. Rosiglitazone further suppresses H3 phosphorylation in comparison with the DMSO control, consistent with the ability of TZDs to induce cell cycle arrest in adipose cells (22). Contrastingly, cells treated with NALs do not show any further suppression of H3 phosphorylation. These data suggest that, compared with agonist ligands (TZDs), NALs preferentially cause apoptotic cell death in response to carboplatin, possibly due to their lack of effect on inhibiting cell cycle progression.

We then examined whether other cell types that expressed PPARγ were also sensitized to the cytotoxic effects of carboplatin. We saw similar effects of these drugs in the mouse Lewis lung carcinoma (LLC) cell lines as coincubation of LLC cells with the TZD pioglitazone or SR1664 with carboplatin increased the accumulation of cleaved PARP1 (Fig. 1*F*). We also assessed the ability of NALs to sensitize MDA-MB-468 cells, a model of triple-negative breast cancer. These cells showed increased phosphorylation of S273 of PPARγ upon treatment with carboplatin (Fig. S1*F*), as well as increased apoptosis with SR1664 cotreatment (Fig. 1*G*), which is quantitated in Fig. S1*D*.

The ability of NALs to sensitize PPARγ-expressing cells is not universal. HCT116 cells, which express high levels of PPARγ

(23), show no significant increased accumulation of cleaved PARP (Fig. S1*E*), and no increased phosphorylation of PPARγ (Fig. S1*G*), suggesting that the sensitization effect of NALs is not present in every cell type despite the presence of PPARγ protein.

We next asked whether the ability of these ligands to sensitize cancer cells to chemotherapeutic cytotoxicity represented a generalized response to DNA damaging agents. We found that A549 cells treated with SR1664 and increasing concentrations of the anthracycline doxorubicin (Fig. 1*H*) and the topoisomerase II inhibitor etoposide (Fig. 1*I*) showed an increased accumulation of cleaved PARP1 compared with DMSO-treated controls. Contrastingly, cotreatment of A549 cells with the microtubule-stabilizing cytotoxic paclitaxel (Fig. S1*H*) did not result in increased cell death. This differential sensitization suggests that inhibition of the phosphorylation of PPARγ genetically sensitizes cells to cytotoxic agents that work directly by damaging the DNA, rather than drugs that are cytotoxic through other mechanisms.

Genetic Inhibition of PPARγ S273 Phosphorylation Mimics the Effects of Noncanonical Agonist PPARγ Ligands on Cell Death. To verify that these results were specifically due to on target effects of inhibition of PPARγ phosphorylation, we used shRNA to generate A549 cells with low levels of PPARγ. Treatment of these cells with SR1664 and carboplatin shows that PPARγ is required for the increased apoptotic cell death (Fig. S1*I*).

To more precisely interrogate the importance of S273 phosphorylation of PPARγ, we took a genetic approach using mice bearing a Ser273→Ala knock-in mutation. We generated immortalized fibroblasts from the brown adipose tissue of these mice (Fig. S1*J*) and treated them with increasing doses of carboplatin. At each dose, from 2.5 μM to 250 μM, there is significantly increased accumulation of both cleaved PARP1 and cleaved Caspase 3 (Fig. 1*J*). These effects are especially striking at 2.5 μM, 10 μM, and 25 μM carboplatin, where there is no significant increase in PARP1 accumulation in the wild-type cells (quantitated in Fig. S1*K*). Thus, abolishing the phosphorylation of PPARγ by mutation of Ser273 to Ala is sufficient to confer a greatly increased sensitivity to apoptotic cell death induced by cytotoxic drugs. This was also true for fibroblasts generated from a separate body site (Fig. S1*L*). Consistent with our data from NAL treatment, we confirmed that these cells are also sensitized to other DNA damaging agents, such as etoposide (Fig. S1*M*) and doxorubicin (Fig. S1*N*), but not taxol (Fig. S1*O*).

Identification of a Core Gene Set Affected by Inhibition of PPARγ S273 Phosphorylation upon Treatment with Carboplatin. To assess the cellular response induced by inhibiting the phosphorylation of PPARγ, we examined global gene expression using Affymetrix arrays (Fig. 2*A*). Upon treatment with carboplatin, 395 genes were down-regulated in mutant cells and 215 genes up-regulated, consistent with the idea that inhibition of S273 phosphorylation results in a profound change in the transcriptome of the cells.

We selected a group of genes that were at least threefold up-regulated with an ANOVA P value < 0.05 for validation. A total of 59 genes (excluding predicted genes and uncharacterized cDNAs) met these criteria and were analyzed (Fig. S2*A*). Forty of these were significantly ($P < 0.05$) regulated in separate experiments (χ^2 $P <$ 0.0063) and multiple others trended toward significance.

We then examined the expression of these genes in other cell types to generate a core signature of PPARγ phosphorylation inhibition after carboplatin treatment. A core set of 12 genes that were up-regulated in the S273A mutant and 11 genes that were down-regulated in the S273A mutant genes was generated based on their expression in multiple cell types with and without carboplatin treatment. Interestingly, most of the down-regulated genes [e.g., *Ptprz1* (24), *Edn1* (25), *Adamts5* (25), *Adm* (26)] have been previously associated with chemotherapy resistance.

This gene set was assessed in A549 cells treated with SR1664 in combination with carboplatin (Fig. 2*B*). Ten of the 12 up-regulated genes were coordinately up-regulated in A549 cells treated with SR1664 and carboplatin. Seven of the 11 genes were

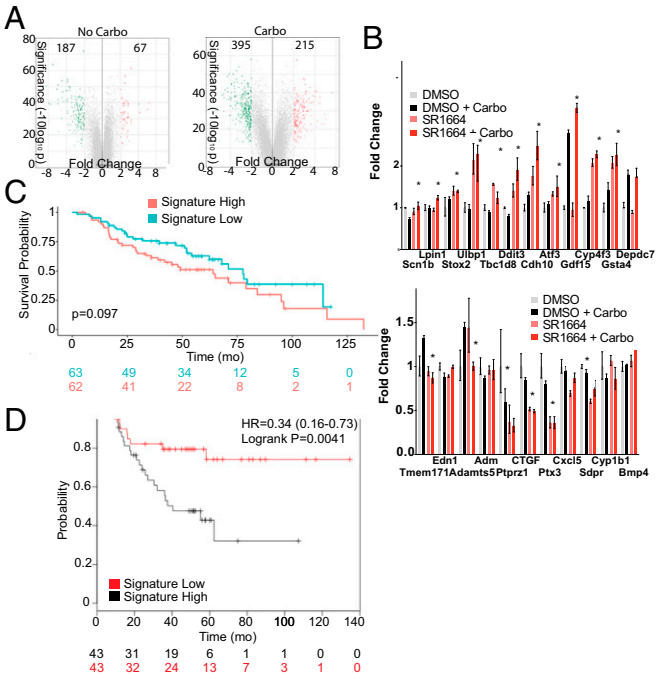

Fig. 2. (*A*) Volcano plots of the comparison between wild-type and knock-in cell gene expression show a threefold increase in the number of differentially regulated genes. (*B*) A core set of genes regulated by S273 phosphorylation in multiple cell types upon carboplatin treatment was generated. Seventeen of a core set of 23 genes were similarly up-regulated (*$P < 0.05$) in A549 lung cancer cells by inhibition of PPARγ phosphorylation with the NAL SR1664 in the presence of carboplatin (χ^2 $P = 0.0218$). (*C*) Kaplan–Meier plot of overall survival over time reveals a trend toward improved survival with high expression of the PPARγ S273A gene signature in the combined cohort of patients receiving adjuvant chemotherapy in the NIH Directors Challenge cohort and the UT Southwestern Lung SPORE cohort. (*D*) Kaplan–Meier analysis of a cohort of 86 ER^-/PR^- breast cancer patients using KMplot revealed a significant difference in recurrence-free survival based on expression of the gene signature.

appropriately down-regulated with SR1664 treatment with carboplatin, for a total of 17 of 23 genes appropriately regulated (χ^2 $P =$ 0.0218). The expression of these genes was also examined in MDA-MB-468 cells treated with SR1664 and carboplatin. We found a similar degree of regulation, although it did not reach significance by chi-square testing (Fig. S2*B*). This core gene set represents a gene-expression–based biomarker of the inhibition of PPARγ phosphorylation in response to carboplatin.

We hypothesized that this gene signature may reflect the sensitivity of tumors to cytotoxic chemotherapy. Using publicly available gene-expression datasets, we queried whether expression of the combined gene set correlated with the outcomes of patients treated with chemotherapy. Patients in the Director's Challenge Consortium (27) who received adjuvant chemotherapy ($n = 90$) and the UT Lung SPORE cohort ($n = 49$) (28), two of the largest cohorts of lung cancer patients receiving adjuvant chemotherapy with available gene-expression data, were classified based on their expression of the genes in the signature. Notably, tissue was obtained before any chemotherapy. Kaplan–Meier analysis of overall survival in these two combined cohorts showed that patients with a greater than median signature score had a trend toward better survival than those who did not express the signature ($P = 0.097$) (Fig. 2*C*). These studies showed a similar trend when analyzed individually as well ($P = 0.1$ and $P = 0.34$) (Fig. S2*C*).

We also examined the gene signature in triple-negative breast cancer using the KMplot online tool (kmplot.com/analysis/index.php?p=background). Kaplan–Meier analysis of patients with

MEDICAL SCIENCES

estrogen receptor-negative/progesterone receptor-negative (ER^-/PR^-) breast cancers treated with chemotherapy showed that expression of the gene signature was associated with a significantly increased recurrence-free survival (median 58.15 mo vs. 21 mo) with a hazard ratio (HR) of 0.34 ($P = 0.0041$) (Fig. 2*D*). Interestingly, analysis of patients who did not receive chemotherapy shows that there was no difference in recurrence-free survival among the groups (Fig. S2*D*), suggesting that the gene signature does not simply reflect prognosis, but rather is predictive of chemotherapy response. A similar analysis of patients with lung cancer treated with chemotherapy showed a trend for improved outcomes with a HR of 0.27 ($P = 0.0507$) (Fig. S2*E*), although the analysis was limited by the small number of patients ($n = 34$). Of course, these analyses are limited due to the mixed clinical and pathologic features of these cohorts. However, these data suggest that low expression of the down-regulated genes and high expression of the up-regulated genes is associated with improved outcomes among patients receiving systemic chemotherapy.

Noncanonical Agonist PPARγ Ligands Synergize Effectively with Carboplatin in Vivo. We next investigated whether inhibition of PPARγ phosphorylation could be a therapeutic target in vivo. We first examined short-term treatment of lung tumors in animals bearing a Lox-Stop-Lox mutant KRAS allele driven by inhaled adenoviral Cre (29). We treated animals with established lung tumors with carboplatin plus either rosiglitazone, SR1664, or vehicle for 2 d. Tumors were subjected to TUNEL staining for apoptotic cells, or immunohistochemistry for accumulation of γ-H2AX, a key marker of DNA damage. There was a significant increase in the number of $\gamma\text{-H2AX}^+$ cells in animals treated both with rosiglitazone and with SR1664 when combined with carboplatin (Fig. 3*A*). There was also a significant increase in the number of $TUNEL^+$ cells per field examined, increasing from 5% in controls to 10% with rosiglitazone and 12% for SR1664 (Fig. 3*B*) ($P < 0.001$). These data suggest that the inhibition of S273 phosphorylation of PPARγ is a bona fide therapeutic target, and that NALs can sensitize lung cancer cells to carboplatin in vivo.

It was obviously important to investigate the effects of long-term therapeutic treatment of animals with these ligands. Tumor xenografts of A549 cells were grown in the flanks of nude mice and randomly assigned into treatment groups with vehicle, vehicle + carboplatin, pioglitazone, pioglitazone + carboplatin, SR1664, or SR1664 + carboplatin. Tumors from animals treated with SR1664 and carboplatin were significantly smaller than tumors from animals treated with vehicle and carboplatin alone. This trend was evident after about 2 wk of treatment, and became statistically significant by 30 d and remained so through the end of the experiment (Fig. 3*C*). These data were replicated in an independent experiment that showed essentially the same results (Fig. S3*B*). Tumor weights were measured from this second experiment (Fig. 3*D*) and confirmed that the SR1664/carboplatin group tumors weighed significantly less than those treated with vehicle/carboplatin ($P = 0.016$). Tumors from animals treated with SR1664/carboplatin trended toward being smaller than those from animals treated with pioglitazone/carboplatin ($P = 0.058$).

To verify that our treatment was affecting the S273 phosphorylation of PPARγ, we analyzed expression of the core gene set altered by inhibition of PPARγ phosphorylation in the presence of carboplatin (Fig. S4*C*). Sixteen of the 23 genes that were identified in our gene set were coordinately regulated in the appropriate direction (χ^2 $P = 0.06$), suggesting that the xenografts were indeed responding to the effects of inhibition of PPARγ phosphorylation.

PPARγ Phosphorylation Plays a Role in the Response to DNA Damage. Although our prior data implicated metallothionein gene expression as a potential mechanism for the sensitization of TZDs to the effects of carboplatin, the broader effects of NALs with DNA damaging agents suggests a more general mechanism must be at work. Furthermore, treatment of A549 cells with NALs did not affect metallothionein gene expression (Fig. S4*A*). To assess

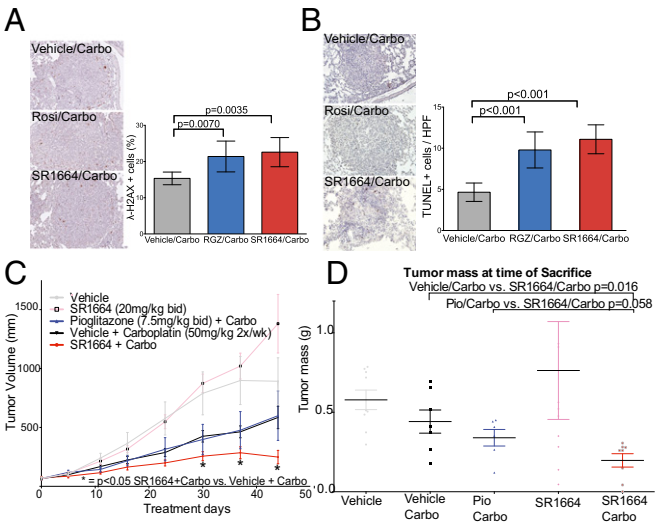

Fig. 3. (*A* and *B*) Aperio analysis of γ-H2AX staining (*A*) and TUNEL staining (*B*) in sections from tumors in lungs of inducible KRAS G12D allele activated with inhaled adenoviral Cre. An increase in labeled cells was seen with cotreatment of animals with both rosiglitazone and SR1664 compared with vehicle and carboplatin alone. (Magnification: 200×.) (*C*) Graph of xenograft volumes over time from a representative experiment. Tumors on animals treated with SR1664 and carboplatin were significantly smaller than those treated with vehicle and carboplatin. Tumors from animals treated with pioglitazone were not statistically smaller than those from control carboplatin animals, although this effect was due to a single outlier, as evidenced by the results when the data were transformed to a modified mean (Fig. S3*A*). (*D*) Tumor weights at the time of killing of mice from a separate experiment of nude mice with A549 cell xenografts treated with the indicated drugs ($n = 7$–10). There was a significant difference in tumor weight of xenografts in mice treated with SR1664 compared with those treated with vehicle and carboplatin ($P = 0.016$). The weights of tumors treated with SR1664 and carboplatin were lower than those treated with pioglitazone and carboplatin in a near significant trend ($P = 0.058$).

for potential mechanisms of the increased sensitivity to genotoxic drugs, we performed gene set enrichment analysis (GSEA) using the microarray data generated above (Fig. 4*A*). The most enriched gene set associated with S273A mutation was the p53 pathway (Fig. S4*C*), along with several other DNA damage pathways. This analysis raises the intriguing possibility that the single amino acid change in the S273A knock-in mutants results in alteration of certain aspects of the DNA damage response.

Given the effects on the p53 gene set, we hypothesized that there may be a biochemical interaction between p53 and PPARγ. Immunoprecipitation (IP) of PPARγ from nuclear extracts of wild-type or S273A mutant fibroblasts followed by immunoblotting for p53 demonstrates that the wild-type PPARγ physically associates with p53 while the S273A mutant does not (Fig. 4*B*). This is true both in the presence and the absence of carboplatin, although there is increased association of p53 upon carboplatin treatment. There is no difference in the total levels of PPARγ, and no difference in nuclear accumulation of PPARγ (Fig. S4*B*). These data suggest that phosphorylation of PPARγ stabilizes the interaction of PPARγ and p53, and that mutant PPARγ that cannot be phosphorylated is not able to associate with p53 as efficiently. This differential interaction provides a potential mechanism whereby the blocking the phosphorylation of PPARγ with NALs reduces the interaction with p53 and potentiates apoptotic cell death.

Because p53 plays a central role in coordinating the DNA damage response, we next examined the effects of inhibition of S273 phosphorylation on markers of the DNA damage response. A549 cells treated with the NALs SR1664 and SR1824 showed increased accumulation of S1981 phospho-ATM (Fig. 4*C*) and

A

Hallmark Gene Set	Size	ES	NES	NOM p-val	FDR q-val	FWER p-val	Rank at Max
p53 Pathway	193	0.63	2.4	0	0	0	2603
Xenobiotic Metabolism	197	0.5	1.94	0	0	0.001	3248
Interferon Alpha Response	89	0.54	1.89	0	0	0.001	2533
Bile Acid Metabolism	110	0.47	1.69	0	0.007	0.033	3494
Apoptosis	155	0.42	1.58	0.001	0.026	0.152	1706
Heme Metabolism	182	0.38	1.47	0.006	0.071	0.437	4178
Interferon Gamma Response	195	0.38	1.46	0.008	0.072	0.495	2533
UV Response Up	143	0.38	1.43	0.014	0.08	0.564	3924
ROS Pathway	44	0.44	1.39	0.072	0.112	0.717	5660
IL6 Jak Stat Signaling	87	0.39	1.37	0.041	0.131	0.808	1861
Peroxisome	99	0.37	1.33	0.059	0.17	0.9	3355
Hypoxia	191	0.33	1.28	0.06	0.237	0.972	2131
DNA Repair	137	0.34	1.26	0.096	0.262	0.99	4835
Hedgehog Signaling	36	0.42	1.25	0.178	0.259	0.993	1874

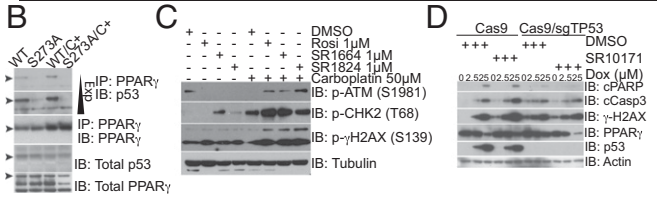

Fig. 4. (*A*) Table from GSEA of the microarray gene-expression data generated from wild-type vs. S273A fibroblasts treated with carboplatin was performed using the Hallmark gene sets. (*B*) IP of endogenous PPARγ and immunoblots for p53 reveals a preferential association between wild-type PPARγ and p53 compared with the S273A mutant. (*C*) Western blotting of lysates harvested from A549 cells show accumulation of markers of the activated DNA damage response. (*D*) CRISPR/Cas9-mediated deletion of TP53 abrogates the ability of NALs to sensitize A549 cells to doxorubicin.

increased phosphorylation of Chk2 T68, both markers of increased DNA damage signaling. Interestingly, increased accumulation of γ-H2AX, a marker of DNA double-strand breaks, was also seen. Thus, cells treated with NALs and genotoxic agents show an increased amount of unrepaired DNA damage.

We hypothesized that the interaction of p53 and PPARγ may play an important role in the ability of NALs to sensitize cancer cells to DNA damage. We examined the effects of NALs in combination with carboplatin in Calu-1 cells, which have deletion of p53 (Fig. S4*F*), as well as H2009 cells, which express mutant p53 (Fig. S4*D*). In both cell types, we fail to see an increase in the DNA damage marker γ-H2AX when cells are treated with both SR1664 and carboplatin. Ectopic expression of wild-type p53 in Calu-1 cells rescued the ability of SR1664 to sensitize cells to the DNA damage produced by carboplatin (Fig. S4*F*). These data suggest that the presence of wild-type p53 is required for the sensitizing effects of NALs.

To further investigate the role of p53 in the ability of NALs to sensitize cells to DNA damaging agents, we performed CRISPR/Cas9-mediated deletion of TP53 from A549 cells. Control cells transduced with Cas9 alone show robust increases in cleaved PARP and cleaved Caspase 3 when treated with the NAL SR10171 and doxorubicin compared with doxorubicin alone (Fig. 4*D*, lane 3 vs. lane 6). Contrastingly, cells depleted of p53 show no significant increase in accumulation of apoptotic markers or γ-H2AX phosphorylation when cotreated with SR10171 and doxorubicin. We also confirmed these results using shRNA-mediated knockdown of TP53 from A549 cells (Fig. S4*E*). These data suggest that p53 is required for the ability of NALs to sensitize cells to genotoxic agents.

Discussion

We have shown that NALs are able to sensitize cancer cells to DNA damaging agents in vitro and in vivo. Our data show that PPARγ is phosphorylated upon exposure to DNA damage, and inhibition of this phosphorylation results in increased DNA damage and tumor cell death. Taken together, these data indicate that PPARγ is a very promising target for cancer-directed therapy, and that modulation of S273 phosphorylation may provide a wider therapeutic window than conventional agonist ligands.

These data show that cell-autonomous effects of NALs cause increased apoptosis in response to DNA damaging agents, but the magnitude of the effects in vivo seem to be larger than the effects seen on fractional cell growth in vitro. It is possible that there may be additional effects of NALs on other cell types in the tumor microenvironment, including immune cells that may play a significant role in impacting tumor growth in vivo.

We have demonstrated that mutation of a single amino acid of PPARγ results in a profound change in the response of fibroblasts to a variety of DNA damaging agents. Our data suggest a model where phosphorylation of PPARγ is a cellular response to DNA damage, and this nuclear receptor then aids in the repair response via p53. Inhibition of phosphorylation by NALs disrupts the PPARγ/p53 interaction, resulting in increased DNA damage, which triggers apoptotic cell death. To the best of our knowledge, PPARγ has not been known to be involved in DNA repair or in the response to DNA damaging agents. At this point, we have not identified the kinase responsible for PPARγ phosphorylation. It is reasonable to suspect that one of any number of kinases involved in the DNA damage response (e.g., DNA-PK, ATM, or ATR) might be involved. However, the S273 site is not within a consensus motif for these PI3K family members, making this possibility less likely. However, this site can be phosphorylated both by ERK (14) and CDK5 (13), both of which can be activated by DNA damage (30, 31). Additional studies are needed to clarify which of these kinases play a role in PPARγ phosphorylation.

These data suggest that this therapeutic strategy would be best adopted in p53 wild-type tumors, which accounts for ∼50% of human cancers. Our data also imply that expression of the S273A gene signature is associated with a trend toward improved outcomes after chemotherapy in multiple cancer types. Because these samples were taken before chemotherapy, the differences in gene expression among samples suggest that there may be phosphorylation occurring in tumors at baseline. We hypothesize that tumor inflammation, ongoing DNA damage, or other factors may result in phosphorylation of PPARγ in some tumors, which results in low expression of the gene signature. Direct interrogation of phosphorylation in tumors via better phospho-specific antibodies or mass spectrometry would also help clarify the extent of PPARγ phosphorylation in vivo. We believe that the patients most likely to show a synergy with NALs and chemotherapy would be those with tumors with a low signature score. Treatment with NALs might boost expression of the gene signature by inhibiting phosphorylation and sensitize those tumors to adjuvant chemotherapy. Of course, such an approach would need to be tested in a prospective manner.

To our knowledge, this work is unique in reporting an interaction between PPARγ and the tumor suppressor P53. We have shown via IP that wild-type PPARγ can interact with p53, while the S273A mutant is unable to bind. This interaction may be direct, or may be indirect in a larger protein complex. Further characterization of this interaction may yield insights into which aspects of p53 biology are specifically being affected by PPARγ. Interestingly, p53 has been show to play a role in adipose tissue inflammation (32), a scenario where PPARγ is also phosphorylated. Our observations raise the possibility that the PPARγ/p53 interaction may also play an important role in adipose tissue biology.

One intriguing aspect of this work is that the induction of markers of apoptosis is much greater with SR1664 compared with rosiglitazone. One potential explanation for this change is due to their differential effects on cell cycle progression. In general, cells confronted with genotoxic stress can either arrest at some stage of the cell cycle and attempt repair or initiate apoptotic cell death. One function of conventional agonist PPARγ ligands like TZDs is to cause cell cycle arrest (22) as part of its prodifferentiation program. The NALs do not appear to influence mitotic progression. Thus, cells treated with these drugs do not arrest the cell cycle, perhaps allowing for continued division in the face of DNA damage, triggering apoptotic cell death. Consistent with that theory, there was a trend toward increased tumor control in xenografts treated with SR1664 compared with

TZDs, although this did not achieve statistical significance. Additional studies appropriately powered to detect these differences may provide further insight into the differential efficacy of these drugs.

In this study, we have shown activity of PPARγ ligands in combination with DNA damaging agents in nonsmall cell lung cancer as well as triple-negative breast cancer. However, PPARγ is expressed in a variety of other cancers, including 22% of colorectal cancer, (33) and 71% of pancreatic cancers (34). However, PPARγ has been largely overlooked as a potential therapeutic in cancer, likely due to the controversies surrounding the black box warning for rosiglitazone as well as failure in nonbiomarker driven clinical studies (35). Of course, not all tumor cells (e.g., HCT116 colorectal cells) are sensitized by NALs, which may result from any combinations of low expression levels of PPARγ, lack of phosphorylating kinases, poor drug penetration, or efflux pumps that limit effective drug concentrations. However, we believe that these data suggest that targeting PPARγ phosphorylation may be a valuable therapeutic approach applicable in combination with a wide variety of genotoxic agents directed toward many different cancer types.

Experimental Procedures

Detailed methods for reagents, antibodies, cell culture, qPCR, protein analysis, and microarray analysis are provided in *SI Experimental Procedures*.

Animal Experiments. All animal experiments were approved by the Institutional Animal Care and Use Committee of the Beth Israel Deaconess Medical Center. Six- to 10-wk-old nude male mice were randomly assigned to treatment groups of: vehicle, vehicle + carboplatin (50 mg/kg, Monday, Wednesday, and Friday), pioglitazone (7.5 mg/kg, twice a day) + carboplatin, SR1664 (20 mg/kg), and SR1664 + carboplatin. Full methods are detailed in *SI Experimental Procedures*.

Microarray Analysis. Full methods of microarray analysis are in *SI Experimental Procedures*. A gene set was defined as genes that were >threefold upregulated with a significant P value (false-discovery rate $P < 0.05$). A refined gene set was generated from these genes with exclusion of genes that were not expressed across a wide variety of cells and tissues. GSEA was performed as described previously (36) using the Hallmark Gene sets defined in the MSigDB.

For analysis of clinical data, raw Affymetrix data and clinical data were downloaded from the Gene Expression Omnibus (https://www.ncbi.nlm.nih.gov/geo) for the NIH Director's Challenge's study (27) and the UT Lung Spore Cohort (28), along with the clinical data. A gene signature score reflecting greater or less than median gene expression was defined. The association of signature classification with survival was analyzed using the Kaplan–Meier method in R studio. As an alternative approach, we used the online tool KMplot (kmplot.com/analysis/index.php?p=background) to analyze data for breast cancer (37).

Statistics. Student's test was used for single comparisons of mean values. Error bars represent ± SEM except when otherwise specified. A two-way ANOVA was used to compare multiple groups. A chi-square test was used to compare gene expression changes in the gene set. An asterisk (*) indicates $P < 0.05$ except when specified.

ACKNOWLEDGMENTS. We thank Dr. Pere Puigserver, Dr. Rana Gupta, Dr. David Miyamoto, and Dr. Evan Rosen for helpful comments, as well as constructive comments from members of the B.M.S. laboratory. This work was supported by National Cancer Institute–Massachusetts General Hospital Federal Share Program NCI-C06-CA-059267 (to M.J.K.); Department of Defense Lung Cancer Research Program Career Development Award LC140129 (to M.J.K.); NIH Grants DK31405 (to B.M.S.) and DK107717 (to A.S.B.); and the JPB Foundation (B.M.S.).

1. Tontonoz P, Hu E, Spiegelman BM (1994) Stimulation of adipogenesis in fibroblasts by PPAR gamma 2, a lipid-activated transcription factor. *Cell* 79:1147–1156.
2. Lehmann JM, et al. (1995) An antidiabetic thiazolidinedione is a high affinity ligand for peroxisome proliferator-activated receptor gamma (PPAR gamma). *J Biol Chem* 270:12953–12956.
3. Kroll TG, et al. (2000) PAX8-PPARgamma1 fusion oncogene in human thyroid carcinoma [corrected]. *Science* 289:1357–1360; erratum in (2000) 289:1474.
4. Sarraf P, et al. (1999) Loss-of-function mutations in PPAR gamma associated with human colon cancer. *Mol Cell* 3:799–804.
5. Mueller E, et al. (1998) Terminal differentiation of human breast cancer through PPAR gamma. *Mol Cell* 1:465–470.
6. Mueller E, et al. (2000) Effects of ligand activation of peroxisome proliferator-activated receptor gamma in human prostate cancer. *Proc Natl Acad Sci USA* 97: 10990–10995.
7. Smith MR, et al. (2004) Rosiglitazone versus placebo for men with prostate carcinoma and a rising serum prostate-specific antigen level after radical prostatectomy and/or radiation therapy. *Cancer* 101:1569–1574.
8. Burstein HJ, et al. (2003) Use of the peroxisome proliferator-activated receptor (PPAR) gamma ligand troglitazone as treatment for refractory breast cancer: A phase II study. *Breast Cancer Res Treat* 79:391–397.
9. Girnun GD, et al. (2008) Regression of drug-resistant lung cancer by the combination of rosiglitazone and carboplatin. *Clin Cancer Res* 14:6478–6486.
10. Girnun GD, et al. (2007) Synergy between PPARgamma ligands and platinum-based drugs in cancer. *Cancer Cell* 11:395–406.
11. Park J, Morley TS, Scherer PE (2013) Inhibition of endotrophin, a cleavage product of collagen VI, confers cisplatin sensitivity to tumours. *EMBO Mol Med* 5:935–948.
12. Soccio RE, Chen ER, Lazar MA (2014) Thiazolidinediones and the promise of insulin sensitization in type 2 diabetes. *Cell Metab* 20:573–591.
13. Choi JH, et al. (2010) Anti-diabetic drugs inhibit obesity-linked phosphorylation of PPARgamma by Cdk5. *Nature* 466:451–456.
14. Banks AS, et al. (2015) An ERK/Cdk5 axis controls the diabetogenic actions of PPARγ. *Nature* 517:391–395.
15. Marciano DP, et al. (2015) Pharmacological repression of PPARgamma promotes osteogenesis. *Nat Commun* 6:7443.
16. Choi JH, et al. (2011) Antidiabetic actions of a non-agonist PPARγ ligand blocking Cdk5-mediated phosphorylation. *Nature* 477:477–481.
17. Khandekar MJ, Cohen P, Spiegelman BM (2011) Molecular mechanisms of cancer development in obesity. *Nat Rev Cancer* 11:886–895.
18. Hirsch HA, Iliopoulos D, Tsichlis PN, Struhl K (2009) Metformin selectively targets cancer stem cells, and acts together with chemotherapy to block tumor growth and prolong remission. *Cancer Res* 69:7507–7511.
19. Goodwin PJ, et al. (2011) Evaluation of metformin in early breast cancer: A modification of the traditional paradigm for clinical testing of anti-cancer agents. *Breast Cancer Res Treat* 126:215–220.
20. Shackelford DB, et al. (2013) LKB1 inactivation dictates therapeutic response of nonsmall cell lung cancer to the metabolism drug phenformin. *Cancer Cell* 23:143–158.
21. Jiralerspong S, et al. (2009) Metformin and pathologic complete responses to neoadjuvant chemotherapy in diabetic patients with breast cancer. *J Clin Oncol* 27: 3297–3302.
22. Altiok S, Xu M, Spiegelman BM (1997) PPARgamma induces cell cycle withdrawal: Inhibition of E2F/DP DNA-binding activity via down-regulation of PP2A. *Genes Dev* 11:1987–1998.
23. Dai Y, et al. (2009) Peroxisome proliferator-activated receptor-gamma contributes to the inhibitory effects of Embelin on colon carcinogenesis. *Cancer Res* 69:4776–4783.
24. Fu F, et al. (2016) Expression of receptor protein tyrosine phosphatase ζ is a risk factor for triple negative breast cancer relapse. *Biomed Rep* 4:167–172.
25. Lloyd KL, Cree IA, Savage RS (2015) Prediction of resistance to chemotherapy in ovarian cancer: A systematic review. *BMC Cancer* 15:117.
26. Lopez-Ayllon BD, et al. (2014) Cancer stem cells and cisplatin-resistant cells isolated from non-small-lung cancer cell lines constitute related cell populations. *Cancer Med* 3:1099–1111.
27. Shedden K, et al.; Director's Challenge Consortium for the Molecular Classification of Lung Adenocarcinoma (2008) Gene expression-based survival prediction in lung adenocarcinoma: A multi-site, blinded validation study. *Nat Med* 14:822–827.
28. Tang H, et al. (2013) A 12-gene set predicts survival benefits from adjuvant chemotherapy in non-small cell lung cancer patients. *Clin Cancer Res* 19:1577–1586.
29. Jackson EL, et al. (2001) Analysis of lung tumor initiation and progression using conditional expression of oncogenic K-ras. *Genes Dev* 15:3243–3248.
30. Tian B, Yang Q, Mao Z (2009) Phosphorylation of ATM by Cdk5 mediates DNA damage signalling and regulates neuronal death. *Nat Cell Biol* 11:211–218.
31. Tang D, et al. (2002) ERK activation mediates cell cycle arrest and apoptosis after DNA damage independently of p53. *J Biol Chem* 277:12710–12717.
32. Minamino T, et al. (2009) A crucial role for adipose tissue p53 in the regulation of insulin resistance. *Nat Med* 15:1082–1087.
33. Ogino S, et al. (2009) Colorectal cancer expression of peroxisome proliferator-activated receptor gamma (PPARG, PPARgamma) is associated with good prognosis. *Gastroenterology* 136:1242–1250.
34. Kristiansen G, et al. (2006) Peroxisome proliferator-activated receptor gamma is highly expressed in pancreatic cancer and is associated with shorter overall survival times. *Clin Cancer Res* 12:6444–6451.
35. Shaw AT, et al. (2012) Randomized phase 2 study of efatutazone in combination with carboplatin and paclitaxel as first-line therapy for metastatic nonsmall cell lung cancer (NSCLC). *Proceedings of the 103rd Annual Meeting of the American Association for Cancer Research* (American Association for Cancer Research, Philadelphia), Abstract 4606.
36. Mootha VK, et al. (2003) PGC-1alpha-responsive genes involved in oxidative phosphorylation are coordinately downregulated in human diabetes. *Nat Genet* 34:267–273.
37. Győrffy B, et al. (2010) An online survival analysis tool to rapidly assess the effect of 22,277 genes on breast cancer prognosis using microarray data of 1,809 patients. *Breast Cancer Res Treat* 123:725–731.

Supporting Information

Khandekar et al. 10.1073/pnas.1717776115

SI Experimental Procedures

Reagents. Rosiglitazone and pioglitazone were purchased from Sigma. SR1664, SR1824, SR10171, and MRL-24 were synthesized at Scripps Florida, as previously described (1, 2). Doxorubicin, carboplatin, taxol, and etoposide for cell culture experiments were purchased from Sigma. Pharmaceutical grade carboplatin for animal experiments was purchased from Patterson Veterinary.

Antibodies. Antibodies were obtained from Cell Signaling unless otherwise specified. The PPARγ IP experiments were performed using E-8 antibody from Santa Cruz. The phospho-specific antibody to pS273 PPARγ has previously been described (3).

Cell Culture. To generate immortalized fibroblasts, interscapular brown adipose stromal vascular fraction was obtained from 4-wk-old mice with the following genotypes: $Pparg^{wt/wt}$ or $Pparg^{S273A/S273A}$. Interscapular brown adipose was dissected, washed in PBS, minced, and digested for 45 min at 37 °C in PBS containing 1.5 mg/mL collagenase B (Roche), 123 mM NaCl, 5 mM KCl, 1.3 mM $CaCl_2$, 5 mM glucose, 100 mM Hepes, and 4% essentially fatty acid-free BSA. Tissue suspension was filtered through a 40-μm cell strainer and centrifuged at 600 × *g* for 5 min to pellet the fibroblastic cells. The cell pellet was resuspended in DMEM+ 10% FBS and plated. After 3 d of culture, a fibroblastic culture was obtained. These cells were then infected with lentivirus containing SV40 (abm). Cells were verified for infection by RT-PCR for SV40 viral antigens. These cells were maintained in DMEM+10% FBS.

For lentiviral experiments, 293T cells were transfected with Fugene 6 (Roche) with viral vectors and supernatants harvested after 48 h. shRNA and scramble constructs were obtained from the Dana Farber Cancer Institute RNA Interference Screening Facility. Cells were infected for 24 h, and analyzed 24 h after infection was completed.

RT-PCR. RNA was extracted from cultured cells or frozen tissue samples using TRIzol (Invitrogen), purified with Qiagen RNeasy minicolumns and reverse-transcribed using a High Capacity cDNA Reverse Transcription kit (Applied Biosystems). Resulting cDNA was analyzed by qRT-PCR. Briefly, 25 ng of cDNA and 150 nmol of each primer were mixed with SYBR GreenER PCR Master Mix (Invitrogen). Reactions were performed in 384-well format using an ABI PRISM 7900HT instrument (Applied Biosystems). Relative mRNA levels were calculated using the comparative CT method normalized to TATA binding protein mRNA.

IP and Western Blotting. For IP, crude nuclear extracts were prepared from confluent cells grown on 15-cm plates. Cells were washed with PBS, scraped, and pelleted by centrifugation at 4°. Cells were resuspended in buffer (20 mM Tris, 100 mM NaCl, 300 mM Sucrose, 3 mM $MgCl_2$) and incubated on ice for 10 min. Cells were centrifuged at 900 × *g* at 4°. The pellet was resuspended in 187 μL of nuclear extraction buffer (20 mM Tris, 100 mM NaCl, 2 mM EDTA) and the volume was measured. A volume of 5 M NaCl was added to the solution to bring the total concentration of NaCl to 0.42 M, and the solution was pipetted vigorously. Pellets were incubated on ice for 30 min with occasional mixing, and then spun at maximum speed for 20 min at 4°. Protein was quantified for SDS/PAGE using a BCA assay (Pierce). For IP, 1 g of nuclear extract protein was diluted in buffer containing 50 mM Tris, 1% Igepal CA-360, 10% glycerol, and the final concentration of NaCl was adjusted to 150 mM. PPARγ was immunoprecipitated with antibody overnight, and antigen/antibody complexes were collected using Dynabeads Protein G (ThermoFisher) and a magnetic rack. Beads were washed five times with the IP buffer, and elution was performed using NuPage LDS buffer with 2.5% β-mercaptoethanol and boiling for 5 min. Samples were run on NuPage SDS gells with Mops buffer and Western blotting performed as described previously (3). For conventional Western blotting, samples were collected and lysed in RIPA buffer and run on NuPage SDS gels, as described above.

Animal Experiments. All animal experiments were approved by the Institutional Animal Care and Use Committee of the Beth Israel Deaconess Medical Center. Mice (*Mus musculus*) were maintained in 12-h light/dark cycles (6:00 AM–6:00 PM) at 24 °C. Nude mice were purchased from Taconic and maintained in autoclaved cages with irradiated diet that had also been autoclaved. Six- to 10-wk-old male mice were used for xenograft experiments. Preliminary data suggested groups of 8–10 mice were appropriate to achieve sufficient power to detect a difference between DMSO treatment and treatment with SR1664. Xenografts were generated by injecting 5×10^6 cells in DMEM media into the flank. Tumor dimensions were measured twice weekly using tumor calipers and converted to volume using the formula $V = (\pi \times \text{length}) \times (\text{width}^2/6)$. Treatment was started once tumors measured 50–75 mm^3 were present on the flank. Animals were randomly assigned to treatment groups of: vehicle, vehicle + carboplatin (50 mg/kg, Monday, Wednesday, and Friday), pioglitazone (7.5 mg/kg, twice a day) + carboplatin, SR1664 (20 mg/kg), and SR1664 + carboplatin. Mice were weighed daily for dosing. Treatment drugs were dissolved in vehicle containing DMSO, Cremophor EL, and sterile saline. Drugs were delivered via intraperitoneal injection twice a day. Carboplatin or sterile saline was delivered via intraperitoneal injection on Monday, Wednesday, and Friday.

Microarray Analysis. RNA was harvested and hybridization performed by the Dana Farber Cancer Institute Molecular Biology Core Facilities. Affymetrix Mouse Gene 2.0 ST chips were used. Data were analyzed using Affymetrix Expression Console software and Transcriptome Analysis Console. A gene set was defined as genes that were >threefold up-regulated with a significant *P* value (false-discovery rate $P < 0.05$). These were validated in separate qPCR experiments using cDNA from fibroblasts. A refined gene set was generated from these genes with exclusion of genes that were not expressed across a wide variety of cells and tissues. GSEA was performed as described (4) using the Hallmark Gene sets defined in the MSigDB.

For analysis of clinical data, raw Affymetrix data were downloaded from the Gene Expression Omnibus (https://www.ncbi.nlm.nih.gov/geo) for the NIH Director's Challenge's study (5) and the UT Lung Spore Cohort (6), along with the clinical data. Patients who did not receive adjuvant chemotherapy were excluded. Affymetrix data were normalized using RMA in R (RStudio 1.0.143). The probe IDs associated with the genes in the gene signature were identified. If any genes were not represented in the array used, it was discarded. The median gene expression of each probe ID was calculated. To generate a classifying statistic, for genes that were down-regulated by S273A mutation, patients with gene expression less than the median

were assigned a value of 1, while those who had a gene expression greater than the median had a value of 0. Conversely, for genes that were up-regulated by S273A mutation, patients whose gene expression was greater than the median were assigned a value of 1 and those whose value was less than the median were 0. These values were summed and the median value of the classifier statistic was calculated. Patients whose classifying statistic was greater than the median were defined as having a positive signature, while those less than the median were defined as having a negative signature. The association of signature classification with survival was analyzed using the survfit function, and a Kaplan–Meier plot was generated using ggplot2 in RStudio. Significance was calculated using log-rank test using the survdiff function.

As an alternative approach, we used the online tool KMplot (kmplot.com/analysis/index.php?p=background) to analyze data for breast cancer (7). We restricted our analysis to patients with ER^-/PR^- cancers who received adjuvant chemotherapy and used their multigene classifier with the down-regulated genes weighted as −1 and the up-regulated genes weighted as 1. Patients were split at the median, and recurrence-free survival was analyzed. A similar analysis was carried out excluding patients who received systemic chemotherapy. Analysis of lung cancer patients for overall survival was undertaken with a similar approach.

Microscopy. Tumors or lungs were removed from animals and fixed with 4% paraformaldehyde followed by dehydration in 70% ethanol before embedding. Tissues were embedded in paraffin by the Rodent Histopathology Core at Harvard Medical School. Immunohistochemistry was performed as described previously (8). TUNEL staining was performed using the Apoptag Peroxidase in Situ Apoptosis Detection Kit (EMD Millipore) per the manufacturer's instructions. Images were acquired containing the entire tissue section, and analyzed using the Aperio Imagescope Software, which was performed by the Dana Farber/Harvard Cancer Center Research Pathology Core.

Statistics. Student's test was used for single comparisons of mean values. Error bars represent ± SEM except when otherwise specified. Two-way ANOVA was used to compare multiple groups. A chi-square test was used to compare gene expression changes in the gene set. An asterisk (*) indicates $P < 0.05$ except when specified.

1. Choi JH, et al. (2011) Antidiabetic actions of a non-agonist PPARγ ligand blocking Cdk5-mediated phosphorylation. *Nature* 477:477–481.
2. Stechschulte LA, et al. (2016) PPARG post-translational modifications regulate bone formation and bone resorption. *EBioMedicine* 10:174–184.
3. Choi JH, et al. (2010) Anti-diabetic drugs inhibit obesity-linked phosphorylation of PPARgamma by Cdk5. *Nature* 466:451–456.
4. Mootha VK, et al. (2003) PGC-1alpha-responsive genes involved in oxidative phosphorylation are coordinately downregulated in human diabetes. *Nat Genet* 34: 267–273.
5. Shedden K, et al.; Director's Challenge Consortium for the Molecular Classification of Lung Adenocarcinoma (2008) Gene expression-based survival prediction in lung adenocarcinoma: a multi-site, blinded validation study. *Nat Med* 14:822–827.
6. Tang H, et al. (2013) A 12-gene set predicts survival benefits from adjuvant chemotherapy in non-small cell lung cancer patients. *Clin Cancer Res* 19:1577–1586.
7. Győrffy B, et al. (2010) An online survival analysis tool to rapidly assess the effect of 22,277 genes on breast cancer prognosis using microarray data of 1,809 patients. *Breast Cancer Res Treat* 123:725–731.
8. Lo JC, et al. (2014) Adipsin is an adipokine that improves β cell function in diabetes. *Cell* 158:41–53.

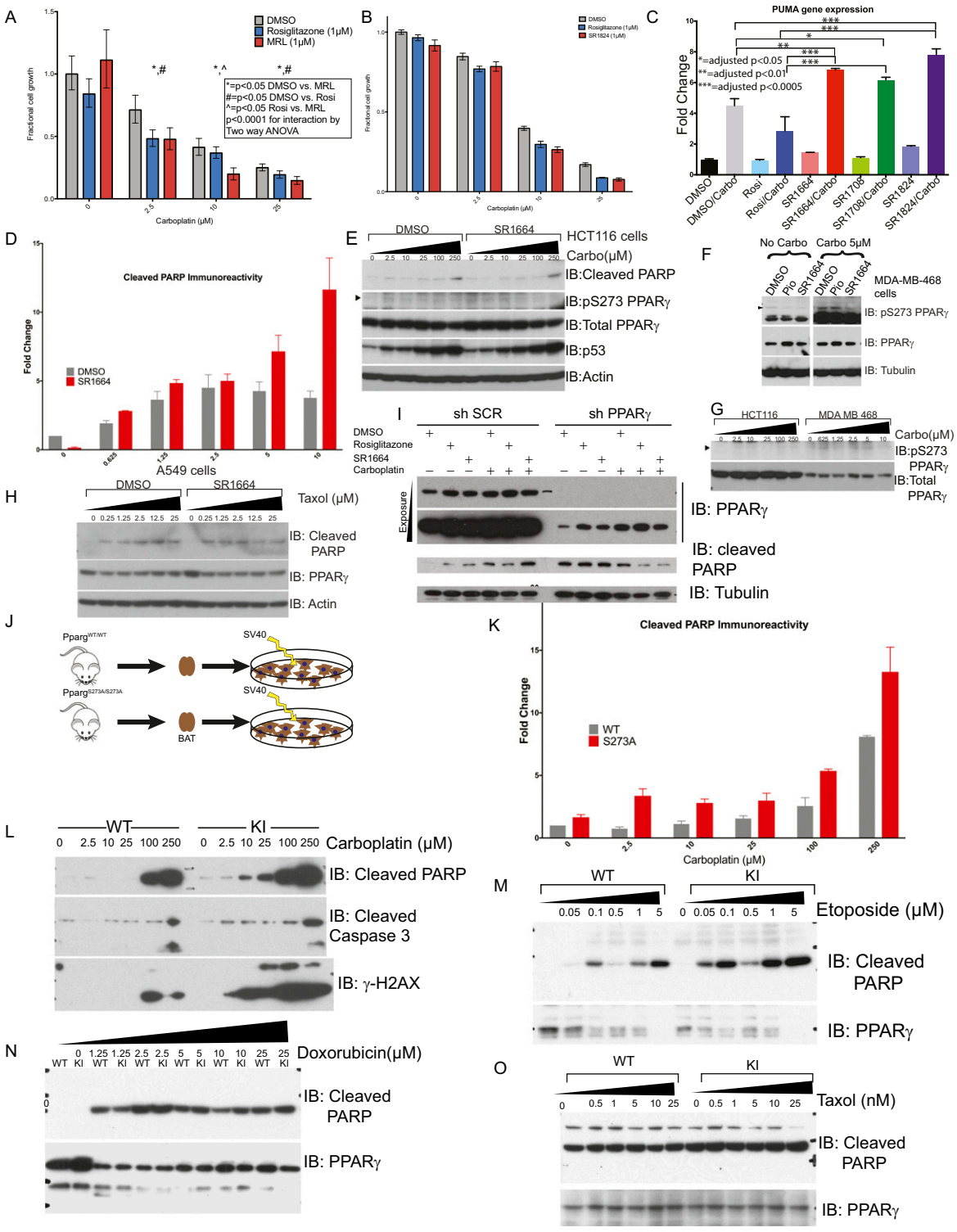

Fig. S1. (*A*) Treatment of A549 cells with other nonagonist PPARγ ligands with increasing concentrations shows similar effects on cell growth as rosiglitazone. The effect of MRL-24, a partial agonist, in combination with carboplatin is shown. There is a significant decrease in cell growth with cells treated with MRL-24 compared with all tested concentrations. (*B*) Cotreatment of A549 cells with SR1824, another noncanonical agonist ligand, with carboplatin also shows a sensitization effect at all concentrations tested. There was no difference in the effects of rosiglitazone and the nonagonist or partial agonist ligands. (*C*) Increase in PUMA gene expression with cotreatment of A549 cells with NALs. (*D*) Densitometric quantitation of cleaved PARP immunoreactivity of MDA-MB-468 cells treated in duplicate with SR1664 and carboplatin. Figures were analyzed in ImageJ and normalized to tubulin, then compared with the signal from the DMSO/untreated sample. Graph shows the mean ± SEM. (*E*) HCT116, a colorectal cancer line, are not sensitized to the effects of carboplatin by SR1664. There is no apparent increase in phosphorylation of PPARγ in this cell type, despite increases in accumulation of p53 in these cells upon treatment with carboplatin. (*F*) MDA-MB-468 cells also show phosphorylation of PPARγ on S273, which can be inhibited by the nonagonist ligand SR1664. Whole-cell lysates from cells were prepared after 24-h treatment with 5 μM carboplatin and cotreatment with the indicated drugs. Panels were from separate lanes of the same gel and blot. (*G*) Blot of pS273-PPARγ and total PPARγ from HCT116 cells (lanes 1–6) and MDA-MB-468 cells (lanes 7–12) treated with increasing concentration of carboplatin. Notably, the cells have difference IC50s for carboplatin, and thus different doses are used. HCT116 cells show minimal increase in phosphorylated PPARγ despite having significantly more total PPARγ than MDA-MB-468 cells. (*H*) A549 cells treated with paclitaxel and SR1664 do not show any increased apoptosis, in contrast to DNA damage directed chemotherapeutics. (*I*) Knockdown of PPARγ eliminates the sensitization of A549 cells to the combination of SR1664 and carboplatin. Cells infected with scrambled shRNA lentivirus continue to show increased PARP cleavage when treated with SR1664 and carboplatin. A lentiviral shRNA for PPARγ knocks down the protein level significantly (*Left* side), and abolishes the increase in cleaved PARP1 seen with the combination of SR1664 and carboplatin (*Right* side). (*J*) Schematic of our immortalization of fibroblasts generated from the brown adipose tissue (BAT) of mice bearing a homozygous knock in mutation of S273→A. (*K*) Densitometric quantitation of cleaved PARP immunoreactivity of BAT preadipocytes from wild-type or S273A KI genetic backgrounds treated in triplicate with increasing doses of carboplatin. Blots were analyzed in ImageJ and compared with the signal from the DMSO/untreated sample. Graph shows the mean ± SEM. (*L*) Treatment of fibroblasts derived from inguinal white adipose tissue (WAT) from wild-type and knock-in mice show a similar effect as those from BAT. Fibroblasts from inguinal WAT were isolated and immortalized using SV40 lentivirus. Wild-type and knock-in mutant fibroblasts were treated with increasing concentrations of carboplatin for 24 h. Whole-cell lysates were probed with the indicated antibodies. There was a significant increase in the accumulation of the markers of apoptosis, cleaved PARP1, and cleaved caspase 3. There was also increased accumulation of DNA damage, as evidenced by the increase in γ-H2AX. (*M*) Knock-in fibroblasts are more sensitive to the cytotoxic effects of etoposide, the topoisomerase II inhibitor. (*N*) These effects are also demonstrated with the anthracycline doxorubicin. (*O*) There is no apparent sensitization of S273A knock-in cells to the microtubule stabilizing chemotherapeutic paclitaxel.

1. Tontonoz P, Hu E, Spiegelman BM (1994) Stimulation of adipogenesis in fibroblasts by PPAR gamma 2, a lipid-activated transcription factor. *Cell* 79:1147–1156.
2. Lehmann JM, et al. (1995) An antidiabetic thiazolidinedione is a high affinity ligand for peroxisome proliferator-activated receptor gamma (PPAR gamma). *J Biol Chem* 270:12953–12956.
3. Kroll TG, et al. (2000) PAX8-PPARgamma1 fusion oncogene in human thyroid carcinoma [corrected]. *Science* 289:1357–1360; erratum in (2000) 289:1474.
4. Sarraf P, et al. (1999) Loss-of-function mutations in PPAR gamma associated with human colon cancer. *Mol Cell* 3:799–804.
5. Mueller E, et al. (1998) Terminal differentiation of human breast cancer through PPAR gamma. *Mol Cell* 1:465–470.
6. Mueller E, et al. (2000) Effects of ligand activation of peroxisome proliferator-activated receptor gamma in human prostate cancer. *Proc Natl Acad Sci USA* 97:10990–10995.
7. Smith MR, et al. (2004) Rosiglitazone versus placebo for men with prostate carcinoma and a rising serum prostate-specific antigen level after radical prostatectomy and/or radiation therapy. *Cancer* 101:1569–1574.
8. Burstein HJ, et al. (2003) Use of the peroxisome proliferator-activated receptor (PPAR) gamma ligand troglitazone as treatment for refractory breast cancer: A phase II study. *Breast Cancer Res Treat* 79:391–397.
9. Girnun GD, et al. (2008) Regression of drug-resistant lung cancer by the combination of rosiglitazone and carboplatin. *Clin Cancer Res* 14:6478–6486.
10. Girnun GD, et al. (2007) Synergy between PPARgamma ligands and platinum-based drugs in cancer. *Cancer Cell* 11:395–406.
11. Park J, Morley TS, Scherer PE (2013) Inhibition of endotrophin, a cleavage product of collagen VI, confers cisplatin sensitivity to tumours. *EMBO Mol Med* 5:935–948.
12. Soccio RE, Chen ER, Lazar MA (2014) Thiazolidinediones and the promise of insulin sensitization in type 2 diabetes. *Cell Metab* 20:573–591.

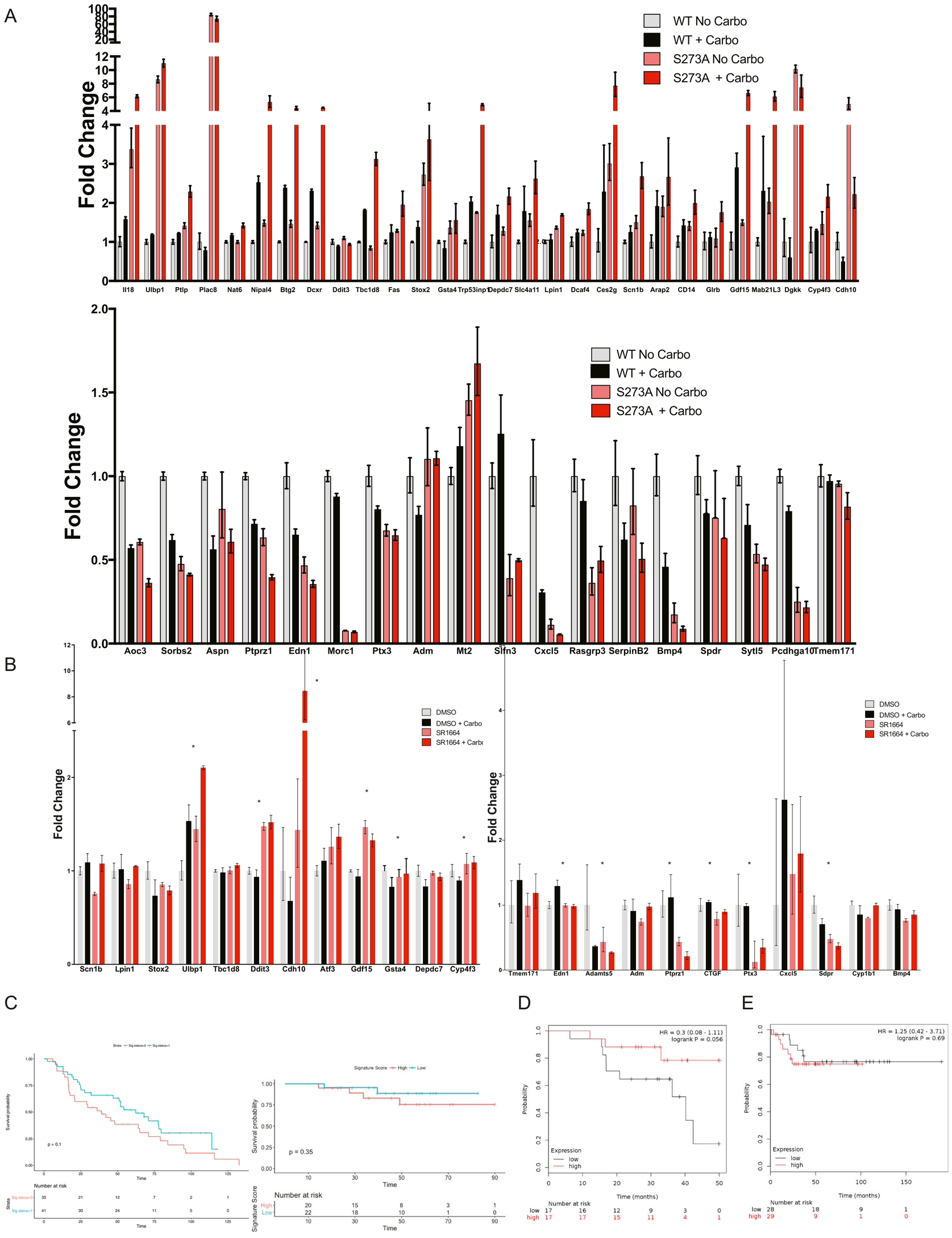

Fig. S2. (*A*) Validation of the genes most differentially expressed between wild-type and knock-in cells treated with carboplatin. Forty of 59 genes were appropriately regulated in the mutant cells treated with carboplatin compared with wild-type controls (χ^2 $P = 0.0063$). (*B*) MDA-MB-468 cells were treated with SR1664 and carboplatin or controls. RNA was harvested and analyzed by qPCR for the expression of the genes that are up-regulated in the core gene set of PPARγ phosphorylation inhibition. (*Right*) The same cells were analyzed for the core set of genes that are down-regulated upon inhibition of the phosphorylation of PPARγ and carboplatin treatment. *$P < 0.05$. (*C*) Separate analysis of the two cohorts pooled for Fig. 3*D*. For the Director's Challenge (*Left*) and the UT Lung Spore cohort (*Right*), a trend toward improved overall survival based on signature score was seen. (*D*) Kaplan–Meier analysis of ER^-/PR^- patients who did not receive chemotherapy using the KMplot online tool shows no difference in recurrence-free survival based on expression of the PPARγ S273A signature. (*E*) Kaplan–Meier analysis of overall survival of lung cancer patients using the KMplot online tool reveals a trend toward improved survival in patients with expression of the PPARγ S273A signature.

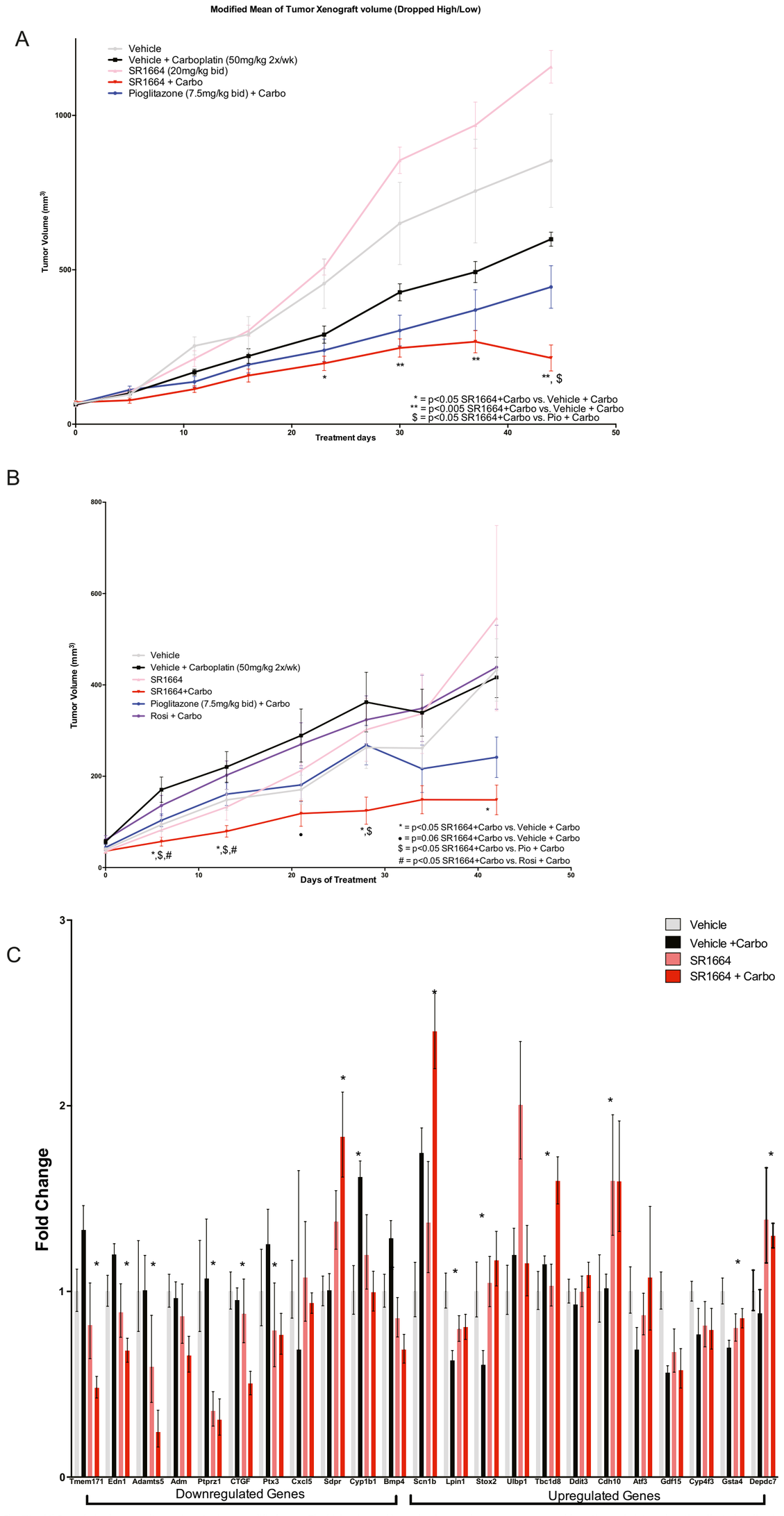

Fig. S3. (*A*) Reanalysis of xenograft experiment using a modified mean. The high value and low value from each group were removed from the analysis to reduce the effect of outliers in the group. The modified mean shows that the effects of both SR1664 and pioglitazone in combination with carboplatin is indeed present and not due to outlier values. (*B*) Graph of tumor volumes over time in a second independent experiment showing that SR1664 and carboplatin treatment is associated with a significantly lower volume compared with DMSO and carboplatin alone. (*C*) Analysis of the gene-expression set indicative of inhibition of PPARγ phosphorylation at S273 in the response to carboplatin suggests the efficacy of SR1664 and carboplatin treatment in the xenografts. Fifteen of 23 genes were regulated in the expected direction (*$P < 0.05$).

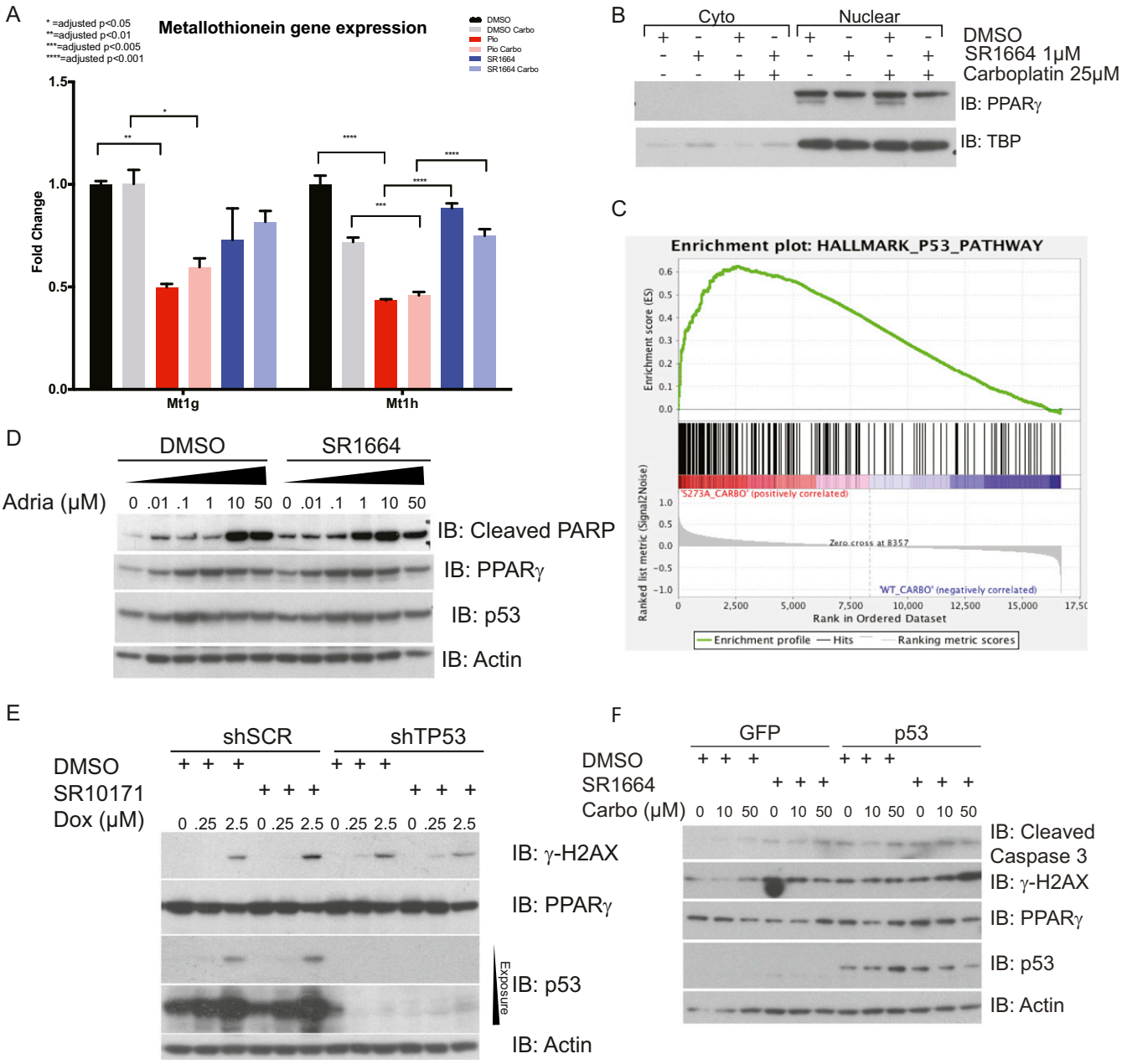

Fig. S4. (*A*) qPCR analysis of two of the metallothionein genes. Treatment of A549 cells with pioglitazone does reduce metallothionein gene expression. However, SR1664 has no effect on metallothionein gene expression, raising the possibility of an alternate mechanism of sensitization. (*B*) Nuclear extracts of A549 cells show no change in total PPARγ nuclear accumulation after treatment with carboplatin or SR1664. (*C*) The top scoring gene set from GSEA, which was enriched in the S273A fibroblasts, was the p53 pathway. (*D*) H2009 cells, which have a mutation in TP53 at codon 273, show no increase in DNA damage as measured by γ-H2AX staining or cell death upon cotreatment of nonagonist ligands and doxorubicin. (*E*) Lentivirally mediated shRNA mediated knockdown of p53 from A549 cells reveals increased sensitization to cytotoxic agents is dependent on p53. Compared with cells infected with a scrambled shRNA, cells with reduced accumulation of P53 due to a p53 shRNA show no increased γ-H2AX production when cells are treated with a nonagonist ligand and doxorubicin. (*F*) NALs do not sensitize p53 null Calu-1 cells to DNA damage from cytotoxic therapy, which can be rescued by reintroduction of wild-type P53.

Dataset S1. List of qPCR primers for PPARγ S273 gene sets

Dataset S1